Doctral Dissertation
博士論文

Effective Theory of Quantum Many-Body Systems Coupled with Mechanical Degrees of Freedom
（力学自由度と結合した量子多体系の有効理論）

A Dissertation Submitted for the Degree of Doctor of Philosophy
December 2020

令和 2 年 12 月 博士（理学）申請
Department of Physics, Graduate School of Science
The Univesity of Tokyo
東京大学大学院理学系研究科物理学専攻

Kentaro Sugimoto
杉本 健太朗

Effective Theory of Quantum Many-Body Systems Coupled with Mechanical Degrees of Freedom

Kentaro Sugimoto

February 21, 2021

Abstract

For many quantum many-body-systems, internal information can be read off as a classical quantity. Based on this idea, this thesis proposes and analyzes two models in which a macroscopic classical-mechanical system and a quantum many-body system are coupled, demonstrating the necessity of modeling the external macroscopic degrees of freedom for the study of quantum many-body systems.

The first model focuses on the setup for investigating a two-dimensional helium system with a quartz-crystal microbalance (QCM). This setup is a typical example of a quantum many-body system on a lattice coupled with a classical-mechanically vibrating system. We derive the equation of motion for the QCM as a simplified platform and predict the effects of coupling with two-dimensional ^{4}He. From the results, we find that the effective mass of the entire system, the platform and the ^{4}He atoms, shows a linear increase and a nonlinear depletion with increasing of the ^{4}He atoms. A mean-field approximation also suggests that the latter depletion becomes largest at the half-filling number of ^{4}He atoms.

The second model assumes a magnetic insulator in which the exchange interaction oscillates in time. Since the exchange interaction is responsible for the highest energy scale in magnetic insulators, its experimental realization is difficult. Beyond these difficulties, however, a wide variety of new phenomena

lie ahead. As an example of such a phenomenon, we predict the emergence of long-range interactions and associated initial-state-sensitive dynamics. The initial-state-sensitive dynamics is interesting from our original viewpoint of quantum-classical coupled systems, as it is a sign that classical perturbations from the outside world may cause a large back-action. Analytical and numerical results show that a slight change in the initial state causes a significant difference in the system's time evolution when we drive the exchange interaction with an appropriate amplitude.

Acknowledgments

Contents

Chapter 1

Introduction

1.1 Partially classical open quantum systems

Experimentally probing the microscopic state of quantum many-body systems involves coupling of the quantum system with macroscopic measuring instruments and environments. It is difficult to analyze such setups by investigating isolated quantum systems by means of the Schrödinger equation. This problem has been partly resolved by effectively decoupling the system of interest from the external systems and by measuring it without decoherence. For example, in the imaging of ultracold atoms, various strategies are used to resolve the trade-off between reducing probe-induced atom heating and increasing the imaging resolution [1]. There are also efforts to reduce the quantum back-action associated with measurements in the context of cavity quantum electrodynamics (QED) and that for quantum thermodynamics [2, 3], for example.

On the other hand, some studies actively exploit the inevitable coupling between the system of interest and the external systems. In particular, studies of open quantum systems strongly coupled to external systems has made significant progress in recent years, leading to insights into strong-coupling quantum

thermodynamics [4] and cavity quantum electrodynamics [5, 6]. Studies on driven open quantum systems also have revealed the relation of the injection and the dissipation respectively of energy and particles [7–9].

The above two approaches to quantum many-body systems differ in the way of describing the system: in the former case, one formulates all dynamical variables quantum-mechanically; in the latter case, one can leave truly classical variables as they are. An illustrative example of such classical variables is the electromagnetic field used for trapping cold atoms. Furthermore, many physical quantities measured in experiments are essentially classical. We can interpret, for example, the electric conductivity of a metal or the magnetic moment of a magnet in terms of classical electromagnetic dynamics. In such situations, the latter semi-classical description would be suitable for intuitively understanding phenomena.

We can model such an open quantum system, which partially obeys classical mechanics, as a quantum-classical coupled system as follows; see also Fig. 1.1. First, we have a classical-mechanical system and a quantum one, each obeying an equation of motion individually. Second, we slightly modify each of the equations of motion to incorporate the effects of coupling. The coupling considered here is, for example, electromechanical coupling in piezoelectric materials or magneto-mechanical coupling in ferromagnetic materials. The changes in the equations of motion for the quantum-mechanical system and the classical one correspond to classical-to-quantum perturbation and back-action in the opposite directions, respectively. Interestingly, we can sometimes derive a renormalized equation of motion for the classical-mechanical system by eliminating the dynamical variables for the quantum one. For such a model, this renormalization corresponds to the second-order process through the classical-to-quantum perturbation and the quantum-to-classical back-action.

Such treatment is not always possible, but if it is, it can have a variety of applications. As considered below, graphene and spintronic materials are concrete examples of such a model.

1.1.1 Graphene

Graphene is roughly a coupled system of a classical elastic body following continuum mechanics and a quantum electronic system following the Dirac equation. Through the coupling, elastic deformation creates a gauge field for the electronic system [10–12], and the behavior of the electronic system causes properties of the elastic body to deviate from classical theory [13, 14]. The former mechanism is closely related to strain engineering, which uses elastic deformation to manipulate the electronic properties of graphene [15–17]. The latter mechanism, on the other hand, contributes to the phenomenon of elastic deformation caused by surface plasmons generated by light and other sources, as well as to various related photomechanical effects [18–20].

If we find a renormalized equation of motion for the elastic part of graphene, we can consider various applications. For example, known elastic anomalies [13, 14] in graphene can be fully explained as electron-derived effects. We can also utilize graphene as a controllable actuator by dynamically controlling its elasticity while externally applying an electromagnetic field. It would be even more interesting if additional electromagnetic fields and the elasticity-derived artificial gauge field are coupled nonlinearly.

1.1.2 Spintronics materials

Spintronics materials range from typical magnetic insulators, including ferromagnets and antiferromagnets, to metals and superconductors, and even onto general non-magnetic materials [21–26]. This diversity is due to the variety of

8
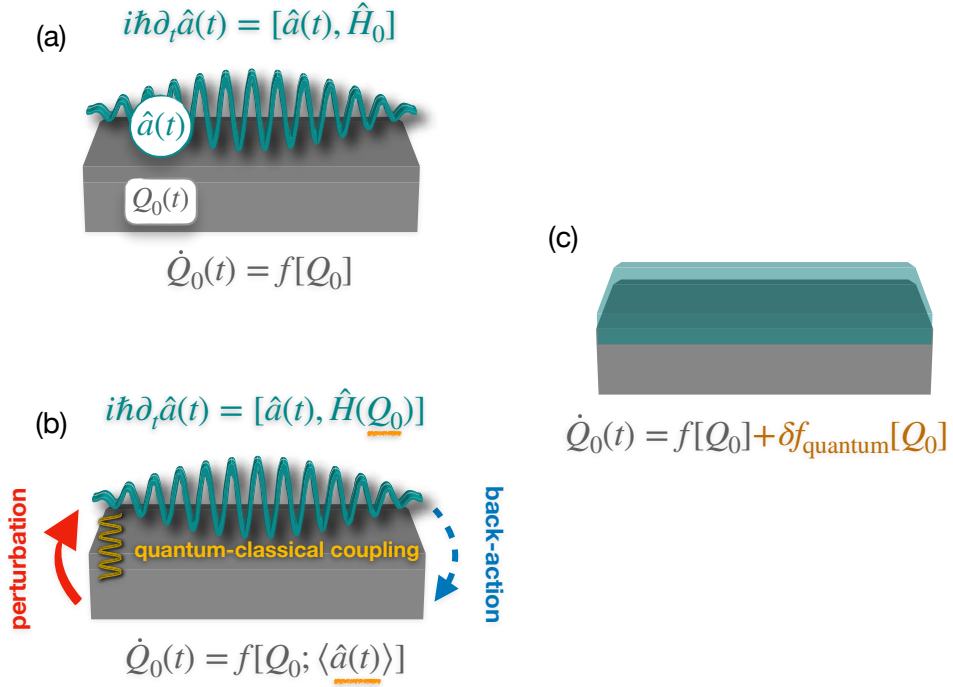
Figure 1.1: Schematic picture of a quantum-classical coupled system. The classical system is characterized by a dynamical variable $Q_0(t)$, while the quantum system is characterized by a dynamical variable $\hat{a}(t)$. (a) A quantum system that obeys the equation of motion $i\hbar\partial_t\hat{a}(t) = [\hat{a}(t),\hat{H}_0]$ and a classical system that obeys the equation of motion $\dot{Q}_0(t) = f[Q_0]$ evolve independently. (b) The classical system and the quantum system are coupled. The Hamiltonian of the quantum system and the time evolution function of the classical system are modified as $\hat{H}_0 \mapsto \hat{H}(Q_0)$ and $f[Q_0] \mapsto f[Q_0; \langle\hat{a}(t)\rangle]$, respectively. Here, the Q_0 dependence of Hamiltonian $\hat{H}_0(Q_0)$ represents the perturbation, while the $\hat{a}(t)$ dependence of the time evolution function $f[Q_0, \langle\hat{a}(t)\rangle]$ represents the back-action. (c) The equation of motion $\dot{Q}_0(t) = f[Q_0] + \delta f_{\text{quantum}}[Q_0]$, where the quantum variables have been eliminated by some procedure and only the classical variables survive. Here, the additional term $\delta f_{\text{quantum}}[Q_0]$ represents the renormalization from the second-order process associated with the coupling to the quantum system.

9

channels through which we can access the electronic spin degrees of freedom in matter. Of particular importance is the mechanical spin-rotation conversion, which utilizes the coupling between the electron's spin degree of freedom and the mechanical rotation, namely the spin-rotation coupling [27]. Mechanical rotation, such as global rotation and elastic deformation, is classical and sometimes macroscopic. Therefore such spintronics materials with classical mechanical degrees of freedom are typical quantum-classical coupled systems.

The mechanism of coupling between electron spins and mechanical rotation in magnetic materials is known as the microscopic origin of the phenomenon of magnetization generation from global rotational motion, formerly known as the Barnett effect [28]. Based on the mechanism, techniques of generating spin current using angular-momentum transfer from the mechanical rotation to electron spins have been proposed [29, 30]. On the other hand, the Einstein-de Haas effect [31], namely the inverse Barnett effect, is known as a fundamental technology of spintronics and has been applied to spin-flip detection with single electron precision [32, 33].

We can also apply the renormalization method to such a mechanically rotating magnetic matter. For example, there is a series of studies of electron spins coupled internally to twisted beam-like elastic bodies [34–36]. In such a system, apart from the spin degree of freedom of the electrons, the beam has an intrinsic torsional rigidity in the bare state. In this case, the electronic spins and the beam torsion are coupled by angular-momentum conservation, and consequently, the beam acquires a renormalized torsional rigidity from a second-order process of the beam-to-spin perturbation and the spin-to-beam back-action. Of course, we need some approximations to eliminate the spin degree of freedom of the electrons. However, this idea may allow us to estimate the energy dispersion of beam-like ferromagnet and antiferromagnet, for

10

example, by measuring the torsional rigidity while applying a magnetic field.

1.2   Scope of this thesis

According to the previous discussion, we can formulate many experimental systems as quantum-classical coupled systems and even describe them classically with fewer degrees of freedom. Reducing the number of degrees of freedom not only saves computational resources but also leads to intuitive understanding. Based on this viewpoint, we first consider two-dimensional ^{4}He on a graphite substrate. Two-dimensional ^{4}He and ^{3}He, along with bulk solid helium, are interesting experimental systems for investigating two-dimensional quantum solids of pure bosons and fermions. Experiments on two-dimensional helium systems have traditionally employed setups of mechanical vibration, such as torsional oscillators (TO) and quartz crystal microbalances (QCM). However, there is still no theory that comprehensively describes such a coupled system. Motivated by this, the present thesis proposes a model of two-dimensional ^{4}He coupled with a macroscopic classical platform.

The concept of quantum-classical coupled system motivates us to investigate yet a new problem. If the quantum system tends to equilibrate autonomously, smaller classical-to-quantum perturbation would generate smaller quantum-to-classical back-action, which is in fact closely related to the relaxation problem of isolated quantum systems [37]. In this case, the scattering process inside the quantum system would not be so complicated. However, if the quantum system has strong initial-state sensitivities, even a small classical-to-quantum perturbation may generate a large quantum-to-classical back-action. In the present thesis, we exploit long-range interactions in spin systems which we show emerge from periodically driven exchange interac-

tions.

The remaining part consist of the following chapters. In Chapter 2, we derive an effective Hamiltonian for two-dimensional ^{4}He coupled to a macroscopic and classical platform, and propose a method of estimating the mass deficit from the associated equation of motion. In Chapter 3, we derive an effective Hamiltonian for a spin system with periodically driven exchange interactions and discuss the emergent long-range interactions as well as strong initial-state sensitivities. Chapter 4 provides a summary, a conclusion, and discussions.

Chapter 2

Hard-core bosons coupled to a platform

2.1   Background and motivation

^{4}He and ^{3}He are bosonic and fermionic isotopes of helium atoms, respectively, and have provided ideal experimental playground for quantum many-body systems [38–40]. Such a quantum nature particularly affects their quantum-solid phases. One example is an elastic anomaly of the bulk solids [41, 42]. Another example is a variety of unusual equilibrium properties in the two-dimensional solids, namely two-dimensional helium, realized on a graphite substrate, e.g. liquid-crystal phase [43], incomplete superfliuidity [44], and commensurate-incommensurate transition [45]. The two-dimensional helium has attracted much attention in recent years for its nanofriction [46–49].

This study is a joint work with Tomoki Minoguchi (Institute of Physics, Univ. Tokyo, as of December 2020) to be submitted (in preparation).

13

In studies on nanofriction in two-dimensional helium, quartz-crystal microbalance (QCM) is often used, as in experimental studies in other film-substrate systems [50–56]. QCM is designed for observing the film's response under mechanical oscillation of the underlying substrate. The force often reaches macroscopic magnitudes, causing decoupling of the film from the substrate. The decoupling invokes an effective change in the total mass, shifting the oscillator's resonant frequency and quality factor. These shifts let us evaluate the film's properties. Such a setup can probe quantum many-body systems without directly observing the quantum many-body system of interest.

The present study aims to theorize such a mechanical-probing setup for quantum systems. To this end, we propose a minimal model of a single-overlayer ^{4}He atoms on a movable platform. Specifically, we consider the small-amplitude limit, in which the overlayer receives only a small effect from the underlying platform, and derive the total effective Hamiltonian with a proper coupling term. The derivation is inspired by the method in Ref. [57]. The effective Hamiltonian yields the platform's equation of motion, by which we obtain an effective-mass formula for the entire system. We organize the remaining sections as follows. Section 2.2 presents a theoretical overview and the results. Section 2.3 gives a summary.

2.2 Methods and Results

2.2.1 Theoretical Overview

In this study, we formulate a situation in which ^{4}He atoms adsorbed on a graphite substrate are coupled globally to a platform which moves under a potential force. This formulation leads to an effective Hamiltonian in the laboratory frame. First, noting that the ^{4}He atoms behave like hard-core bosons

14

(HCB) on a triangular lattice due to the graphite potential and their interparticle repulsions, we describe the ^{4}He atoms on the motionless platform by the following Hamiltonian:

$$\hat{\mathcal{H}}_{\text{HCB}} := -\sum_{(i,j)\in E} J_{i,j}\hat{\mathfrak{a}}_i^\dagger \hat{\mathfrak{a}}_j, \tag{2.1}$$

where E denotes the set of bonds on the triangular lattice, $J_{i,j}$ denotes the transition amplitude at bond (i,j), and $(\hat{\mathfrak{a}}_i, \hat{\mathfrak{a}}_i^\dagger)$ denotes the creation and annihilation operators, respectively, satisfying the following HCB commutation relation:

$$\left[\hat{\mathfrak{a}}_i, \hat{\mathfrak{a}}_j^\dagger\right] = \delta_{i,j}(1 - 2\hat{\mathfrak{n}}_i), \quad \left[\hat{\mathfrak{a}}_i, \hat{\mathfrak{a}}_j\right] = \left[\hat{\mathfrak{a}}_i^\dagger, \hat{\mathfrak{a}}_j^\dagger\right] = 0. \tag{2.2}$$

Here we defined the number operator by $\hat{\mathfrak{n}}_i := \hat{\mathfrak{a}}_i^\dagger \hat{\mathfrak{a}}_i$.

Second, we describe the bare platform subject to a potential force by the following Hamiltonian:

$$\hat{\mathcal{H}}_0 := \frac{\hat{\boldsymbol{P}}_0^2}{2M_0} + V_0(\hat{\boldsymbol{Q}}_0), \tag{2.3}$$

where M_0 denotes the platform mass, $(\hat{\boldsymbol{P}}_0, \hat{\boldsymbol{Q}}_0)$ denote the position and momentum operators of the platform, respectively, with the canonical commutation relation

$$\left[\hat{\boldsymbol{Q}}_0 \overset{\otimes}{,} \hat{\boldsymbol{P}}_0\right] = i\hbar \check{\mathbb{1}}, \tag{2.4}$$

and $V_0(\hat{\boldsymbol{Q}}_0)$ denotes the potential followed by the platform. Here, for any space vectors $\boldsymbol{A} = (A_\mu)$ and $\boldsymbol{B} = (B_\mu)$, and for any operators $\hat{\boldsymbol{C}} = (\hat{C}_\mu)$ and $\hat{\boldsymbol{D}} = (\hat{D}_\mu)$ that work on space vectors, $\boldsymbol{A} \otimes \boldsymbol{B}$ stands for the tensor with $A_\mu B_\nu$ as its (μ, ν) component, and correspondingly, $\left[\hat{\boldsymbol{C}} \overset{\otimes}{,} \hat{\boldsymbol{D}}\right]$ stands for the tensor with $[\hat{C}_\mu, \hat{D}_\nu]$ as its (μ, ν) component. In addition, $\check{\mathbb{1}}$ denotes the identity tensor. In the following, the check symbol on top of a character denotes a tensor.

15

The purpose of this section is to couple the Hamiltonians given by Eqs. (2.1) and (2.3) correctly. The bare platform obeys the following equation of motion for the Hamiltonian $\hat{\mathcal{H}}_0$:

$$\partial_t^2 \hat{\boldsymbol{Q}}_0(t) = -\frac{1}{M_0} V_0'(\hat{\boldsymbol{Q}}_0(t)). \tag{2.5}$$

This is the same as in classical mechanics. However, this equation of motion acquires two additional terms due to the coupling, as we see in the next section:

$$\partial_t^2 \hat{\boldsymbol{Q}}_0(t) \sim -\frac{1}{\mathcal{M}_{\text{tot}}} V_0'(\hat{\boldsymbol{Q}}_0(t)) - \frac{\gamma_N}{i\hbar}\left[\hat{\boldsymbol{V}}_{\text{B}}, V_0(\hat{\boldsymbol{Q}}_0(t))\right] - \gamma_N \hat{\boldsymbol{A}}_{\text{B}}(t), \tag{2.6}$$

where N, m_{B}, and $\mathcal{M}_{\text{tot}} := M_0 + N m_{\text{B}}$ denote the number of particles, the boson mass, and the total mass, respectively. We also denoted that $\gamma_N := N\mu/(1 + N\mu)$. The operators $\hat{\boldsymbol{V}}_{\text{B}}$ and $\hat{\boldsymbol{A}}_{\text{B}}$ denote the collective velocity and collective acceleration of the N-boson system, respectively, which will be defined later. Each of Eqs. (2.5) and (2.6) is an equation of motion for a quantum mechanical operator. We identify the quantum expectation value for each of these equations with that of the platform, which is essentially a classical object. This identification allows us to treat the additional terms in Eq. (2.6) semiclassically.

The strategy for deriving the effective Hamiltonian is as follows. As a primitive model of the HCB model on a lattice, we give an N-boson system interacting in a periodic potential. Here we assume that the potential moves with the platform. This assumption makes it impossible to perform the Wannier-function expansion in the standard way. Therefore, we move to the center-of-mass coordinate of $(N+1)$-particles system of the N bosons and the platform, further even move to a virtual quantum coordinate. These transformations recover the possibility of the Wannier-function expansion. They also play a physical role in effectively decoupling the bosons from the platform. This decoupling produces a small additional term as a side effect, but it is not a prob-

lem. The decoupling also provides mathematical support for the method used in Ref. [57].

2.2.2 Effective Hamiltonian (Result I)

Let us derive the HCB Hamiltonian (2.1) for the bosons on the QCM. We start from the N-boson Hamiltonian by

$$\hat{\mathcal{H}}_{\mathrm{IB}}[\hat{\boldsymbol{Q}}_0] := \sum_{n=1}^{N} \left[\frac{\hat{\boldsymbol{p}}_n^2}{2m_{\mathrm{B}}} + V_{\mathrm{B}}(\hat{\boldsymbol{q}}_n - \hat{\boldsymbol{Q}}_0) \right] + \frac{g}{2} \sum_{n \neq m} \delta(\hat{\boldsymbol{q}}_n - \hat{\boldsymbol{q}}_m), \tag{2.7}$$

where g denotes the interaction strength, and the operators $\{\hat{\boldsymbol{q}}_n\}_{n=1}^{N}, \{\hat{\boldsymbol{p}}_n\}_{n=1}^{N}$ denote the position and momentum of the bosons, respectively, with the following commutation relation:

$$\left[\hat{\boldsymbol{q}}_n \overset{\otimes}{,} \hat{\boldsymbol{p}}_m \right] = i\hbar \delta_{n,m} \breve{\mathrm{I}}. \tag{2.8}$$

Here, $V_{\mathrm{B}}(\hat{\boldsymbol{q}}_n - \hat{\boldsymbol{Q}}_0)$ denotes a periodic potential that moves with the platform position $\hat{\boldsymbol{Q}}_0$. This offset of the potential generates the coupling; see Fig. 2.1. We also assume a lattice structure at the minima of the potential $V_{\mathrm{B}}(\boldsymbol{x})$. For example, in the case of the triangular lattice, we suppose that

$$V_{\mathrm{B}}(\boldsymbol{x}) = \frac{\bar{V}_{\mathrm{B}}}{3} \left\{ 3 - \cos\left[\boldsymbol{k}_1 \cdot \boldsymbol{x}\right] - \cos\left[\boldsymbol{k}_2 \cdot \boldsymbol{x}\right] - \cos\left[(\boldsymbol{k}_1 - \boldsymbol{k}_2) \cdot \boldsymbol{x}\right] \right\} \tag{2.9}$$

with the wave vectors [58–60]

$$\boldsymbol{k}_1 = \frac{2\pi}{\sqrt{3}a}\left(\sqrt{3}, -1\right), \quad \boldsymbol{k}_2 = \frac{4\pi}{\sqrt{3}a}(0, 1), \quad (a: \text{lattice constant}). \tag{2.10}$$

Here, for a set V of sites in the lattice, we only require that $V_{\mathrm{B}}(\boldsymbol{x})$ has a minimum at the position $\boldsymbol{x} = \boldsymbol{x}_i$ of each site $i \in V$. From the above, we have the total Hamiltonian in the form

$$\hat{\mathcal{H}}_{\mathrm{tot}} = \hat{\mathcal{H}}_0 + \hat{\mathcal{H}}_{\mathrm{IB}}[\hat{\boldsymbol{Q}}_0], \tag{2.11}$$

periodic potential $V_B(\hat{\boldsymbol{q}}_n - \hat{\boldsymbol{Q}}_0)$

bosons' position $\hat{\boldsymbol{q}}_1, \hat{\boldsymbol{q}}_2, \cdots$

platform's position $\hat{\boldsymbol{Q}}_0$ $\boldsymbol{x}$
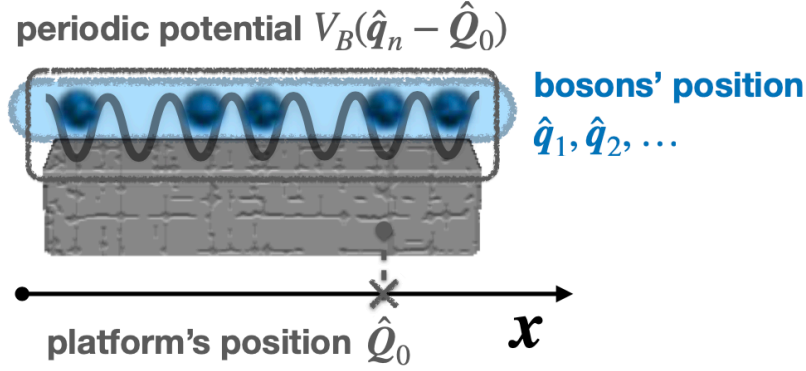
Figure 2.1: Schematic picture of our setup, in which the bosons with the positions $\hat{\boldsymbol{q}}_1, \hat{\boldsymbol{q}}_2, \ldots$ interact in the periodic potential $V_{\mathrm{B}}(\boldsymbol{x})$ in Eq. (2.9) fixed to the platform with the position $\hat{\boldsymbol{Q}}_0$. When the platform moves, the origin of the potential V_{B} moves accordingly, and thus the position of each boson feels shifts from $\boldsymbol{x} = \hat{\boldsymbol{q}}_n$ to $\boldsymbol{x} = \hat{\boldsymbol{q}}_n - \hat{\boldsymbol{Q}}_0$ in the laboratory frame.

where $\hat{\mathcal{H}}_0$ denotes the platform Hamiltonian given in Eq. (2.3).

It would be instructive to derive the HCB Hamiltonian (2.1) on the motionless-platform, namely for the case $\hat{\boldsymbol{Q}}_0 = \boldsymbol{0}$, in the standard prescription. To this end, we start by the Hamiltonian

$$\hat{\mathcal{H}}_{\mathrm{IB}}[\boldsymbol{0}] = \sum_{n=1}^{N} \left[\frac{\hat{\boldsymbol{p}}_n^2}{2m_{\mathrm{B}}} + V_{\mathrm{B}}(\hat{\boldsymbol{q}}_n) \right] + \frac{g}{2} \sum_{n \neq m} \delta(\hat{\boldsymbol{q}}_n - \hat{\boldsymbol{q}}_m). \tag{2.12}$$

In the N-boson symmetrized Hilbert space, the Hamiltonian $\hat{\mathcal{H}}_{\mathrm{IB}}[\boldsymbol{0}]$ can be rewritten as

$$\hat{\mathcal{H}}_{\mathrm{IB}}[\boldsymbol{0}] = \int d\boldsymbol{x}\, \hat{\psi}^\dagger(\boldsymbol{x}) \left[-\frac{\hbar^2 \nabla^2}{2m_{\mathrm{B}}} + V_{\mathrm{B}}(\boldsymbol{x}) \right] \hat{\psi}(\boldsymbol{x}) + \frac{g}{2} \int d\boldsymbol{x}\, \hat{\psi}^\dagger(\boldsymbol{x}) \hat{\psi}^\dagger(\boldsymbol{x}) \hat{\psi}(\boldsymbol{x}) \hat{\psi}(\boldsymbol{x}).$$

$$\tag{2.13}$$

in the second-quantization language. Here we introduced the field operator

$\hat{\psi}(\boldsymbol{x})$ as satisfying

$$[\hat{\psi}(\boldsymbol{x}), \hat{\psi}^\dagger(\boldsymbol{y})] = i\hbar\delta(\boldsymbol{x} - \boldsymbol{y}), \tag{2.14}$$

$$[\hat{\psi}(\boldsymbol{x}), \hat{\psi}(\boldsymbol{y})] = [\hat{\psi}^\dagger(\boldsymbol{x}), \hat{\psi}^\dagger(\boldsymbol{y})] = 0. \tag{2.15}$$

Next, we reduce the Hamiltonian to a lattice model using the Wannier-function expansion. The Wannier-function expansion means rewriting the field operator $\hat{\psi}(\boldsymbol{x})$ in terms of a function $w(\boldsymbol{x}-\boldsymbol{x}_i)$, which is localized at the potential minimum $\boldsymbol{x} = \boldsymbol{x}_i$:

$$\hat{\psi}(\boldsymbol{x}) \simeq \sum_{i\in V} w(\boldsymbol{x} - \boldsymbol{x}_i)\hat{a}_i. \tag{2.16}$$

Here, we also assume that the set of Wannier functions $\{w(\boldsymbol{x} - \boldsymbol{x}_i)\}_{i\in V}$ satisfies an appropriate orthonormality. In addition, $(\hat{a}_i, \hat{a}_i^\dagger)$ denotes the new creation and annihilation operators defined on each site $i \in V$. Using this expansion, we obtain the well-known Bose-Hubbard model [61]:

$$\hat{\mathcal{H}}_{\mathrm{IB}}[\boldsymbol{0}] \simeq - \sum_{(i,j)\in E} J_{i,j}\hat{a}_i^\dagger\hat{a}_j + \frac{U}{2}\sum_{i\in V}\hat{n}_i(\hat{n}_i - 1) \quad (\hat{n}_i := \hat{a}_i^\dagger\hat{a}_i) \tag{2.17}$$

$$=: \hat{\mathcal{H}}_{\mathrm{BH}}, \tag{2.18}$$

where we defined the hopping amplitude by

$$J_{i,j} := \int d\boldsymbol{x}\, w(\boldsymbol{x} - \boldsymbol{x}_i)\left[-\frac{\hbar^2\nabla^2}{2m_{\mathrm{B}}} + V_{\mathrm{B}}(\boldsymbol{x})\right]w(\boldsymbol{x} - \boldsymbol{x}_j) \tag{2.19}$$

and defined the onsite interaction by

$$U := \frac{g}{2}\int d\boldsymbol{x}\, |w(\boldsymbol{x})|^4. \tag{2.20}$$

Here E denotes the set of pairs of neighboring sites (bonds).

Note that the Wannier-function expansion (2.16) holds only if the bosons occupy the lowest band formed by the periodic potential $V_{\mathrm{B}}(\boldsymbol{x})$. In experimental situations, we need to keep the environment temperature sufficiently low

compared to the lowest energy gap. From theoretical viewpoints, this means that we have to choose the initial state from equilibrium states at a sufficiently low temperature when we consider time-evolution problems.

Finally, we take the large-U limit. Under this limit, the HCB commutation relation (2.2) results and the Bose-Hubbard Hamiltonian (2.18) reduces to the HCB Hamiltonian (2.1):

$$\hat{\mathcal{H}}_{\text{BH}} \xrightarrow{U \to \infty} \hat{\mathcal{H}}_{\text{HCB}}. \tag{2.21}$$

The above gives the standard derivation of the HCB model on a lattice (2.1) from interacting bosons in a potential (2.12).

We rewrite the total Hamiltonian $\hat{\mathcal{H}}_{\text{tot}}$ using center-of-mass variables to apply the above prescription even for the case with the platform's motion. To this end, we define new positions by

$$\hat{\mathcal{Q}} := \frac{\hat{\boldsymbol{Q}}_0 + \mu \sum_{n=1}^{N} \hat{\boldsymbol{q}}_n}{1 + N\mu}, \tag{2.22}$$

$$\hat{\boldsymbol{r}}_n := \hat{\boldsymbol{q}}_n - \frac{\hat{\boldsymbol{Q}}_0 + \mu \sum_{n=1}^{N} \hat{\boldsymbol{q}}_n}{1 + N\mu} \quad (n = 1, 2, \dots, N), \tag{2.23}$$

where $\mu := m_{\text{B}}/M_0$ denotes the boson-to-platform mass ratio. Similarly, we define new momenta by

$$\hat{\boldsymbol{\mathcal{P}}} := \hat{\boldsymbol{P}}_0 + \sum_{n=1}^{N} \hat{\boldsymbol{p}}_n, \tag{2.24}$$

$$\hat{\boldsymbol{\pi}}_n := \hat{\boldsymbol{p}}_n - \mu \hat{\boldsymbol{P}}_0 \quad (n = 1, 2, \dots, N). \tag{2.25}$$

These new variables satisfy the following commutation relations as shown in App. 2.B.1:

$$\left[\hat{\boldsymbol{\mathcal{Q}}} \overset{\otimes}{,} \hat{\boldsymbol{\mathcal{P}}} \right] = i\hbar \check{\mathbb{I}}, \tag{2.26}$$

$$\left[\hat{\boldsymbol{r}}_n \overset{\otimes}{,} \hat{\boldsymbol{\pi}}_m \right] = i\hbar \delta_{n,m} \check{\mathbb{I}}. \tag{2.27}$$

Using Eqs. (2.22), (2.23), (2.24), and (2.25) and eliminating the variables $\hat{Q}_0$, $\hat{P}_0$, $\{\hat{q}_n\}$, and $\{\hat{p}_n\}$ yields a new expression given by

$$\hat{\mathcal{H}}_{\text{tot}} = \frac{\hat{\mathcal{P}}^2}{2\mathcal{M}_{\text{tot}}} - \frac{\hat{\mathbf{\Pi}}_B^2}{2\mathcal{M}_{\text{tot}}} + V_0(\hat{\mathcal{Q}} - N\mu\hat{R}_B)$$
$$+ \sum_{n=1}^{N} \left[\frac{\hat{\pi}_n^2}{2m_B} + V_B(\hat{r}_n + N\mu\hat{R}_B) \right] + \frac{g}{2} \sum_{n\neq m} \delta(\hat{r}_n - \hat{r}_m). \qquad (2.28)$$

Here we introduced the new canonical posision and momentum operators

$$\hat{R}_B := \frac{1}{N} \sum_{n=1}^{N} \hat{r}_n, \qquad (2.29)$$

$$\hat{\mathbf{\Pi}}_B := \sum_{n=1}^{N} \hat{\pi}_n \qquad (2.30)$$

with the commutation relation

$$\left[\hat{\mathcal{R}}_B \overset{\otimes}{,} \hat{\mathbf{\Pi}}_B \right] = i\hbar \breve{\mathbb{I}}. \qquad (2.31)$$

The operators $\hat{R}_B$ and $\hat{\mathbf{\Pi}}_B$ capture a collective behavior of the bosons. See also App. 2.B.2 for the derivation.

We need to further transform the Hamiltonian (2.28). Indeed, the argument of $V_B(\hat{r}_n + N\mu\hat{R}_B)$ in Eq. (2.28) differs by $N\mu\hat{R}_B$ from the one in Eq. (2.12), which disables us to apply the Wannier-function expansion straight-forwardly. To fix this difference, we consider a unitary transformation generated by the operator

$$\hat{U}_N := \exp\left[\frac{1}{2} \log\left(1 + N\mu\right)\left(\hat{R}_B \cdot \hat{\mathbf{\Pi}}_B + \hat{\mathbf{\Pi}}_B \cdot \hat{R}_B\right)/i\hbar \right]. \qquad (2.32)$$

This transformation maps the operators $(\hat{r}_n, \hat{\pi}_n, \hat{R}_B, \hat{\mathbf{\Pi}}_B)$ to

$$\hat{U}_N \hat{r}_n \hat{U}_N^\dagger = \hat{r}_n - \frac{N\mu}{1 + N\mu} \hat{R}_B \qquad (2.33)$$

$$\hat{U}_N \hat{\pi}_n \hat{U}_N^\dagger = \hat{\pi}_n + \mu\hat{\mathbf{\Pi}}_B \qquad (2.34)$$

$$\hat{U}_N \hat{R}_B \hat{U}_N^\dagger = \frac{1}{1 + N\mu} \hat{R}_B \qquad (2.35)$$

$$\hat{U}_N \hat{\mathbf{\Pi}}_B \hat{U}_N^\dagger = (1 + N\mu)\hat{\mathbf{\Pi}}_B, \qquad (2.36)$$

and hence maps the Hamiltonian (2.28) to

$$\hat{U}_N \hat{\mathcal{H}}_{\text{tot}} \hat{U}_N^\dagger = \frac{\hat{\mathcal{P}}^2}{2\mathcal{M}_{\text{tot}}} + \frac{\hat{\mathbf{\Pi}}_B^2}{2M_0} + V_0(\hat{\mathcal{Q}} - \gamma_N \hat{\mathbf{R}}_B)$$
$$+ \sum_{n=1}^{N} \left[\frac{\hat{\boldsymbol{\pi}}_n^2}{2m_B} + V_B(\hat{\boldsymbol{r}}_n) \right] + \frac{g}{2} \sum_{n \neq m} \delta(\hat{\boldsymbol{r}}_n - \hat{\boldsymbol{r}}_m); \qquad (2.37)$$

see also Apps. 2.B.3 and 2.B.4 for the derivation. Since the fourth and fifth terms in Eq. (2.37) have the same form as the right-hand side of Eq. (2.12), we can safely perform the Wannier-function expansion and take the large-U limit. Under these procedures for the Hamiltonian (2.37), we finally obtain the effective Hamiltonian

$$\hat{\mathcal{H}}_{\text{eff}} := \frac{\hat{\mathcal{P}}^2}{2\mathcal{M}_{\text{tot}}} + \frac{\hat{\mathbf{\Pi}}_B^2}{2M_0} + V_0(\hat{\mathcal{Q}} - \gamma_N \hat{\mathbf{R}}_B) + \hat{\mathcal{H}}_{\text{HCB}}. \qquad (2.38)$$

Note that the operators $\hat{\mathbf{R}}_B$ and $\hat{\mathbf{\Pi}}_B$ also have the HCB representation:

$$\hat{\mathbf{R}}_B \simeq \frac{1}{N} \sum_{i \in V} \boldsymbol{x}_i \hat{\mathrm{n}}_i, \quad \hat{\mathbf{\Pi}}_B \simeq \sum_{\boldsymbol{k}} \hbar \boldsymbol{k} \, \hat{\mathrm{a}}_{\boldsymbol{k}}^\dagger \hat{\mathrm{a}}_{\boldsymbol{k}}, \qquad (2.39)$$

where $\hat{\mathrm{a}}_{\boldsymbol{k}}$ ($\hat{\mathrm{a}}_{\boldsymbol{k}}^\dagger$) is the Fourier transformation of $\hat{\mathrm{a}}_i$ ($\hat{\mathrm{a}}_i^\dagger$).

In the derivation of Eq. (2.38), we directly applied the discussion from Eq. (2.12) to Eq. (2.21) and replaced the terms

$$\sum_{n=1}^{N} \left[\frac{\hat{\boldsymbol{\pi}}_n^2}{2m_B} + V_B(\hat{\boldsymbol{r}}_n) \right] + \frac{g}{2} \sum_{n \neq m} \delta(\hat{\boldsymbol{r}}_n - \hat{\boldsymbol{r}}_m) \qquad (2.40)$$

by the lattice Hamiltonian $\hat{\mathcal{H}}_{\text{tot}}$ (2.1). To justify this replacement, we must meet the following two conditions, in addition to the one that the environment temperature is sufficiently low:

- The platform's motion does not excite the bosons to higher energy bands of the periodic potential $V_B(\boldsymbol{x})$.

- The Hilbert space of the system is symmetrized with respect to the new variables $\{\hat{\boldsymbol{r}}_n\}_{n=1}^{N}$ introduced in Eq. (2.23).

22

For the first condition to be true, it is essential to keep the *typical frequency* of the platform Ω_0 sufficiently small compared to that of the bosons ω_{B}. Here, the typical frequency of the platform Ω_0 is determined by its maximum acceleration and that of the bosons is given by harmonic approximation of the periodic potential $V_{\text{B}}(\boldsymbol{x})$:

$$\omega_{\text{B}} := \frac{2\pi}{a}\sqrt{\frac{V_0}{m_{\text{B}}}}. \tag{2.41}$$

The second condition above is similar to that for the variables $\{\hat{\boldsymbol{q}}_n\}_{n=1}^{N}$ but is in fact different, since $\{\hat{\boldsymbol{r}}_n\}_{n=1}^{N}$ and $\{\hat{\boldsymbol{q}}_n\}_{n=1}^{N}$ are different variables. In the present case, we can prove that the symmetrization for the variables $\{\hat{\boldsymbol{r}}_n\}_{n=1}^{N}$ is equivalent to that for the variables $\{\hat{\boldsymbol{q}}_n\}_{n=1}^{N}$; see App. 2.C for the proof.

2.2.3   Platform's equation of motion (Result II)

Since we have transformed the original Hamiltonian (2.11) to the one (2.37) by the unitary transformation (2.32), we also have to use the new operator

$$\hat{\boldsymbol{Q}}_{\text{eff}}^{(0)} := \hat{U}_N \hat{\boldsymbol{Q}}_0 \hat{U}_N^\dagger \tag{2.42}$$

$$= \hat{\boldsymbol{Q}} - \gamma_N \hat{\boldsymbol{R}}_{\text{B}} \tag{2.43}$$

to describe the platform's position. With this in mind, we derive the equation of motion for $\hat{\boldsymbol{Q}}_{\text{eff}}^{(0)}(t)$ under the effective Hamiltonian (2.38). Here (t) denotes the argument in the Heisenberg picture, which we omit for brevity in the following. Applying the Heisenberg equation once, we obtain

$$\partial_t \hat{\boldsymbol{Q}}_{\text{eff}}^{(0)} = \frac{\hat{\mathcal{P}}}{\mathcal{M}_{\text{tot}}} - \gamma_N \hat{\boldsymbol{V}}_{\text{B}}, \tag{2.44}$$

where we defined the hardcore boson's collective velocity by

$$\hat{\boldsymbol{V}}_{\text{B}}(t) := \partial_t \hat{\boldsymbol{R}}_{\text{B}}(t). \tag{2.45}$$

23

Defining the platform's effective velocity by $\hat{V}_{\text{eff}}^{(0)} := \partial_t \hat{Q}_{\text{eff}}^{(0)}$ and applying the same again, we arrive at

$$\partial_t \hat{V}_{\text{eff}}^{(0)} = -\frac{1}{\mathcal{M}_{\text{tot}}} V_0'(\hat{\mathcal{Q}} - \gamma_N \hat{R}_{\text{B}}) - \frac{\gamma_N}{i\hbar}\left[\hat{V}_{\text{B}}, V_0(\hat{\mathcal{Q}} - \gamma_N \hat{R}_{\text{B}})\right] - \gamma_N \hat{A}_{\text{B}}, \qquad (2.6)$$

where we defined the hardcore boson's collective acceleration by

$$\hat{A}_{\text{B}}(t) := \partial_t \hat{V}_{\text{B}}(t). \qquad (2.46)$$

Equation (2.6) allows us to predict the motion of the platform coupled to the HCB model for various shapes of the potential $V_0(\hat{Q}_{\text{eff}}^{(0)})$. As a simple example, we consider the case in which a linear force f_{ext} acts on the platform:

$$V_0(\hat{Q}_{\text{eff}}^{(0)}) = -\hat{Q}_{\text{eff}}^{(0)} \cdot f_{\text{ext}}. \qquad (2.47)$$

This assumption yields the following equation:

$$\partial_t \hat{V}_{\text{eff}}^{(0)} = \check{\mathcal{M}}_{\text{eff}}^{-1} \circ f_{\text{ext}} - \gamma_N \hat{A}_{\text{B}}, \qquad (2.48)$$

where we defined the inverse effective-mass tensor by

$$\check{\mathcal{M}}_{\text{eff}}^{-1} := \frac{\check{1}}{\mathcal{M}_{\text{tot}}} + \gamma_N^2 \frac{\left[\hat{R}_{\text{B}} \overset{\otimes}{,} \hat{V}_{\text{B}}\right]}{i\hbar}. \qquad (2.49)$$

The tensor operator $\check{\mathcal{M}}_{\text{eff}}^{-1}$ has a dimension of the inverse mass and gives us information about the response to the applied force f_{ext}. We hence investigate the contribution of the first term $\check{\mathcal{M}}_{\text{eff}}^{-1} \circ f_{\text{ext}}$ in Eq. (2.48). On the other hand, we set aside the discussion of the second term $-\gamma_N \hat{A}_{\text{B}}$ in Eq. (2.48) since its full treatment will require much effort. We believe, however, that linear response theory will allow us to analyze it in the small-f_{ext} limit.

First, we can express the tensor $\check{\mathcal{M}}_{\text{eff}}^{-1}$ explicitly as a function of N:

$$\check{\mathcal{M}}_{\text{eff}}^{-1} = \frac{\check{1}}{M_0 + N m_{\text{B}}} + \left(\frac{N\mu}{1 + N\mu}\right)^2 \check{W}_{\text{B}}, \qquad (2.50)$$

24

where

$$\check{W}_{\mathrm{B}} := \frac{\left[\hat{\boldsymbol{R}}_{\mathrm{B}} \overset{\otimes}{,} \hat{\boldsymbol{V}}_{\mathrm{B}}\right]}{i\hbar}. \tag{2.51}$$

To expand the operator $\check{W}_{\mathrm{B}}$ in fewer terms, we employ the Matsubara-Matsuda transformation [62, 63] and convert the HCB operators to spin-1/2 operators. First, we can rewrite the HCB hamiltonian as

$$\hat{\mathcal{H}}_{\mathrm{HCB}} = -\sum_{(i,j)\in E} J_{i,j}\hat{S}_i^+\hat{S}_j^-, \tag{2.52}$$

where $\{(\hat{S}_i^\pm, \hat{S}_i^z)\}_{i\in V}$ denotes the spin operators with the commutation relation

$$\left[\hat{S}_i^z, \hat{S}_j^\pm\right] = \pm\delta_{i,j}\hat{S}_i^\pm, \quad \left[\hat{S}_i^+, \hat{S}_j^-\right] = 2\delta_{i,j}\hat{S}_i^z. \tag{2.53}$$

The operators $\hat{\boldsymbol{R}}_B$ and $\hat{\boldsymbol{\Pi}}_B$ also acquire the spin-operator representations:

$$\hat{\boldsymbol{R}}_{\mathrm{B}} = \frac{1}{N}\sum_{i\in V}\boldsymbol{x}_i\left(\hat{S}_i^z + \frac{1}{2}\right), \quad \hat{\boldsymbol{\Pi}}_{\mathrm{B}} = \sum_{\boldsymbol{k}}\hbar\boldsymbol{k}\,\hat{S}_{\boldsymbol{k}}^+\hat{S}_{\boldsymbol{k}}^-, \tag{2.54}$$

where $\hat{S}_{\boldsymbol{k}}^\pm$ is the Fourier transformation of $\hat{S}_i^\pm$. Using them, we can explicitly obtain the tensor operator $\check{W}_{\mathrm{B}}$ in the form

$$\check{W}_{\mathrm{B}} = \frac{J}{\hbar^2 N^2}\sum_{(i,j)\in E}(\boldsymbol{x}_i - \boldsymbol{x}_j)\otimes(\boldsymbol{x}_i - \boldsymbol{x}_j)\hat{S}_i^+\hat{S}_j^- + \frac{\check{1}}{M_0}. \tag{2.55}$$

Our next task is to calculate the expectation value of $\check{W}_{\mathrm{B}}$,

$$\langle\check{W}_{\mathrm{B}}\rangle_N = \frac{J}{\hbar^2 N^2}\sum_{(i,j)\in E}(\boldsymbol{x}_i - \boldsymbol{x}_j)\otimes(\boldsymbol{x}_i - \boldsymbol{x}_j)\langle\hat{S}_i^+\hat{S}_j^-\rangle_N + \frac{\check{1}}{M_0}, \tag{2.56}$$

where $\langle\bullet\rangle_N$ denotes the expectation value with respect to the N-boson ground-state. To this end, we first define the quantity

$$\check{\Delta}_N := \frac{1}{a^2|E|}\sum_{(i,j)\in E}(\boldsymbol{x}_i - \boldsymbol{x}_j)\otimes(\boldsymbol{x}_i - \boldsymbol{x}_j)\langle\hat{S}_i^+\hat{S}_j^-\rangle_N, \tag{2.57}$$

25

where a denotes the lattice constant. This gives a dimensionless version of the first term in $\langle \check{W}_{\mathrm{B}} \rangle_N$. Since its exact calculation is diffucult, we numerically estimate the value of $\check{\Delta}_N$ and approximate it by a mean-field solution. Figure 2.2 shows its exact-diagonalization estimate and the mean-field solution given by

$$\check{\Delta}_N \sim \frac{1}{2} \frac{N}{|V|} \left(1 - \frac{N}{|V|} \right) \check{\mathbb{I}}; \tag{2.58}$$

for the derivation of Eq. (2.58), see App. 3.A. Since Eq. (2.58) approximates the numerical estimate shown in Fig. 2.2 well, we deduce that

$$\langle \check{W}_{\mathrm{B}} \rangle_N = \frac{Ja^2}{\hbar^2} \frac{|E|}{N^2} \check{\Delta}_N \tag{2.59}$$

$$\simeq \left[\frac{3}{2} \frac{Ja^2}{\hbar^2} \frac{1}{N} \left(1 - \frac{N}{|V|} \right) + \frac{1}{M_0} \right] \check{\mathbb{I}} \tag{2.60}$$

and that

$$\langle \check{\mathcal{M}}_{\mathrm{eff}}^{-1} \rangle_N = \frac{\check{\mathbb{I}}}{M_0 + N m_{\mathrm{B}}} + \left(\frac{N\mu}{1 + N\mu} \right)^2 \langle \check{W}_{\mathrm{B}} \rangle_N \tag{2.61}$$

$$\simeq \frac{\check{\mathbb{I}}}{M_0} \left[1 - N\mu + \frac{3}{2} \frac{Jm_{\mathrm{B}}a^2}{\hbar^2} \left(1 - \frac{N}{|V|} \right) N\mu \right] + \mathcal{O}(\mu^2). \tag{2.62}$$

Hence its inverse plays the role of the effective mass

$$[\langle \check{\mathcal{M}}_{\mathrm{eff}}^{-1} \rangle_N]^{-1} \simeq \left[M_0 + N m_{\mathrm{B}} - \frac{3}{2} \frac{Jm_{\mathrm{B}}a^2}{\hbar^2} \left(1 - \frac{N}{|V|} \right) N m_{\mathrm{B}} \right] \check{\mathbb{I}}. \tag{2.63}$$

The first two terms in Eq. (2.63) constitute the total mass $\mathcal{M}_{\mathrm{tot}} = M_0 + N m_{\mathrm{B}}$ increasing linearly with N, while the third term indicates a nonlinear depletion with the amplitude $g_{\mathrm{B}} := Jm_{\mathrm{B}}a^2/\hbar^2$. In particular, the depletion is largest in the half-filling case $N/|V| = 1/2$. To see this fact in a μ-independent form, we define the following quantity:

$$\Delta N_{\mathrm{eff}} := \frac{\langle \check{\mathcal{M}}_{\mathrm{eff}} \rangle_N^{x,x} - M_0}{m_{\mathrm{B}}} \tag{2.64}$$

$$\simeq \left[1 - \frac{3}{2} g_{\mathrm{B}} \left(1 - \frac{N}{|V|} \right) \right] N. \tag{2.65}$$
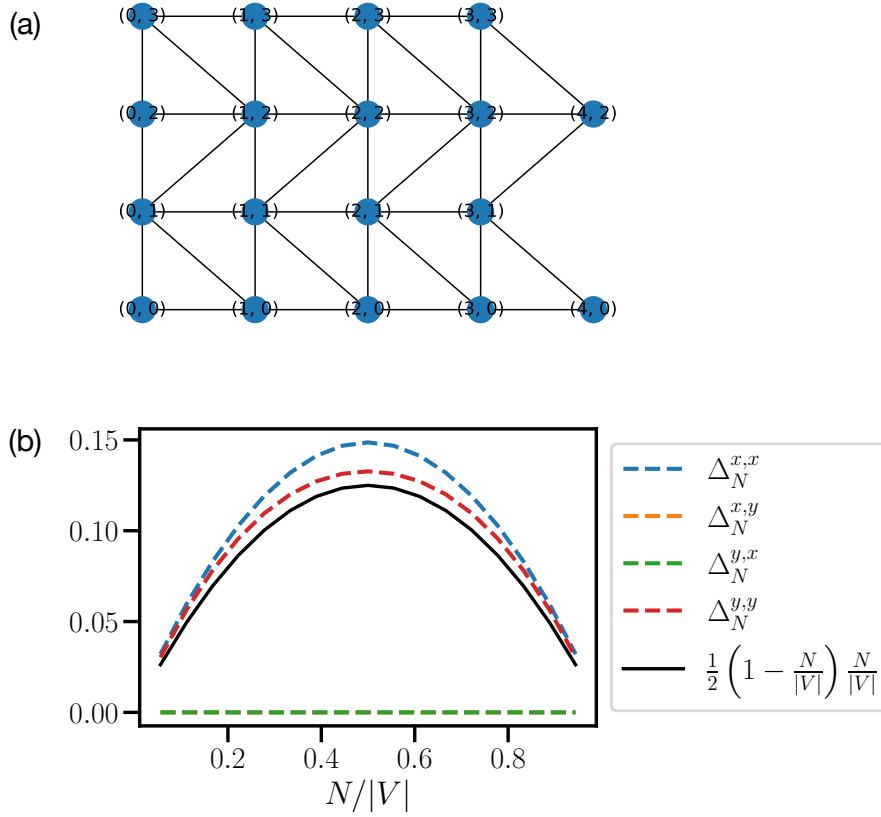
Figure 2.2: (a) Geometry of the triangular lattice used for the numerical calculation. We used the open boundary condition. (b) Numerical results for the matrix elements of $\check{\Delta}_N$ (broken curves) in Eq. (2.57) and the mean-field solution (2.58) (solid curve). The method of numerical calculation is exact diagonalization with QuSpin [64, 65]. Almost only the diagonal component is dominant, with the maximum value around 0.125 both for $\check{\Delta}_N^{x,x}$ and $\check{\Delta}_N^{y,y}$.
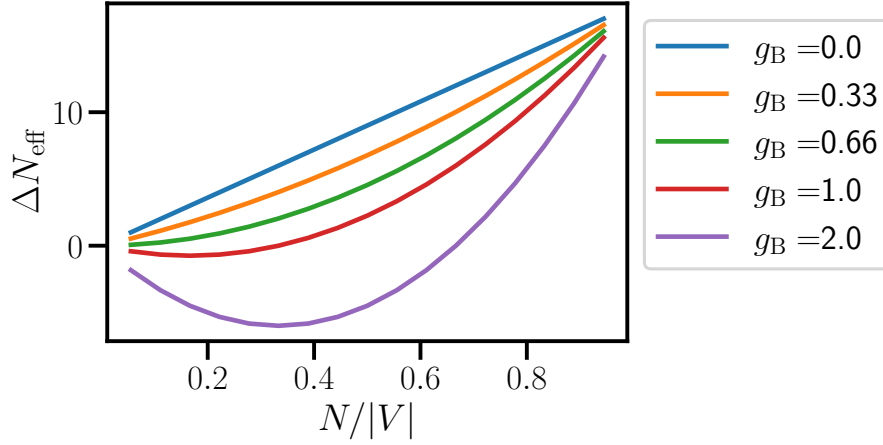
Figure 2.3: The mean-field behavior of ΔN_{eff} at $g_{\text{B}} = 0.0, 0.33, 0.66, 1.0, 2.0$, where $g_{\text{B}} = 0.66 \simeq 2/3$ corresponds to a critical point at which the minimum value of ΔN_{eff} is not less than 0.

The quantity ΔN_{eff} inherits the linear increase term and the nonlinear depletion term in the effective mass $[\langle \check{\mathcal{M}}_{\text{eff}}^{-1} \rangle_N]^{-1}$ in Eq. (2.63), straightforwardly showing the nonlinearity of $[\langle \check{\mathcal{M}}_{\text{eff}}^{-1} \rangle_N]^{-1}$; see also Fig. 2.3. Hence, the effective mass $[\langle \check{\mathcal{M}}_{\text{eff}}^{-1} \rangle_N]^{-1}$ behaves qualitatively the same as the quantity ΔN_{eff}.

2.3   Summary

In this study, we formulated the HCB model on a triangular lattice, which is an effective model of two-dimensional ^{4}He on a movable platform, and derived the effective Hamiltonian (2.38). We also derived the platform's equation of motion (2.6), from which we obtained the effective-mass formula (2.63). The effective-mass formula includes a linearly increasing term and a depletion term as a function of the number of particles.

We have made several assumptions for simplification in this study. First, for a more accurate description of the two-dimensional ^{4}He, we have to adopt

the extended HCB with off-site interaction. The importance of the off-site interaction is also evident from some numerical results showing that ^{4}He atoms on graphite give rise to a non-trivial unit cell [66, 67]. In the analysis of the equations of motion, we have also ignored the term $-\gamma_N \hat{A}_B$. To fully calculate the linear response regime of the external force f_{ext}, we should take this term into account.

Finally, let us discuss the possible variations of this study. Although our original motivation was only to theorize mechanical probing such as QCM, the methods of deriving the effective Hamiltonian and the equation of motion may be applicable to theories of other experimental setups. For example, one idea would be to replace the HCB model with the fermionic Hubbard-type model for the two-dimensional ^{3}He. Another idea would be to replace the simple platform used in this study with an elastically deformable body, which may allow us to consider a deformation of the lattice model.

Appendix

2.A Mean-field approximation of $\check{\Delta}_N$

In this appendix, we derive the mean-field formula

$$\check{\Delta}_N = \frac{1}{a^2 |E|} \sum_{(i,j)\in E} (\boldsymbol{x}_i - \boldsymbol{x}_j) \otimes (\boldsymbol{x}_i - \boldsymbol{x}_j) \langle \hat{S}_i^+ \hat{S}_j^- \rangle_N \tag{2.66}$$

$$\simeq \frac{1}{2} \frac{N}{|V|} \left(1 - \frac{N}{|V|}\right) \check{\mathbf{1}}. \tag{2.57}$$

The derivation requires the following assumptions:

1. The quantity $\langle \hat{S}_i^+ \hat{S}_j^- \rangle_N$ does not depend on the direction of the bond (i,j);

2. The quantity $\langle \hat{S}_i^+ \hat{S}_j^- \rangle_N$ does not depend on the position of the bond (i,j).

The first assumption yields that

$$\langle \hat{S}_i^+ \hat{S}_j^- \rangle_N \simeq \overline{\langle \hat{S}_i^+ \hat{S}_j^- \rangle}_N := \frac{1}{z_G} \sum_{\langle \underline{i}, j\rangle \in E} \langle \hat{S}_i^+ \hat{S}_j^- \rangle_N, \quad \text{for } i \in V, \tag{2.67}$$

where $\sum_{\langle \underline{i}, j\rangle \in E}$ denotes taking the sum of the bonds j connected to i by the bonds in the set E and z_G denotes the coordination number (degree) of the lattice $G = (V, E)$. In the case of the triangular lattice, $z_G = 6$. Using this, we can show that

$$\sum_{\langle \underline{i}, j\rangle \in E} (\boldsymbol{x}_i - \boldsymbol{x}_j) \otimes (\boldsymbol{x}_i - \boldsymbol{x}_j) \langle \hat{S}_i^+ \hat{S}_j^- \rangle_N \simeq 3a^2 \overline{\langle \hat{S}_i^+ \hat{S}_j^- \rangle}_N \check{\mathbf{1}}. \tag{2.68}$$

30

Adding the second assumption yields the following

$$\overline{\langle \hat{S}_i^+ \hat{S}_j^- \rangle}_N \simeq \frac{1}{|E|} \sum_{\langle i,j \rangle \in E} \langle \hat{S}_i^+ \hat{S}_j^- \rangle_N =: \rho_N, \tag{2.69}$$

where ρ_N denotes the spin stiffness. We can also approximate the spin stiffness ρ_N by the order parameter at zero temperature as follows:

$$\rho_N = \frac{1}{|E|} \sum_{\langle i,j \rangle \in E} \langle \hat{S}_i^+ \hat{S}_j^- \rangle_N \simeq \frac{1}{|V|} \sum_{i \in V} |\langle \hat{S}_i \rangle_N|^2 =: \left[|\psi|^2 \right]_N, \tag{2.70}$$

where $\left[|\psi|^2 \right]_N$ denotes the order parameter. The above discusson and the mean-field solution

$$\left[|\psi|^2 \right]_N = \frac{N}{|V|} \left(1 - \frac{N}{|V|} \right) \tag{2.71}$$

for the hard-core boson [68] yields

$$\overline{\langle \hat{S}_i^+ \hat{S}_j^- \rangle}_N \simeq \frac{N}{|V|} \left(1 - \frac{N}{|V|} \right). \tag{2.72}$$

Substituting Eqs. (2.68), (2.72) and the general relation $|E| = 3|V|$ for the triangular lattice $|E| = 3|V|$, we finally obtain

$$\check{\Delta}_N = \frac{1}{a^2 |E|} \sum_{(i,j) \in E} (\boldsymbol{x}_i - \boldsymbol{x}_j) \otimes (\boldsymbol{x}_i - \boldsymbol{x}_j) \langle \hat{S}_i^+ \hat{S}_j^- \rangle_N \tag{2.73}$$

$$= \frac{1}{2a^2 |E|} \sum_{i \in V} \left[\sum_{(i,j) \in E} (\boldsymbol{x}_i - \boldsymbol{x}_j) \otimes (\boldsymbol{x}_i - \boldsymbol{x}_j) \langle \hat{S}_i^+ \hat{S}_j^- \rangle_N \right] \tag{2.74}$$

$$\simeq \frac{1}{2a^2 |E|} \sum_{i \in V} \left(3a^2 \overline{\langle \hat{S}_i^+ \hat{S}_j^- \rangle}_N \check{1} \right) \tag{2.75}$$

$$= \frac{1}{2|V|} \sum_{i \in V} \overline{\langle \hat{S}_i^+ \hat{S}_j^- \rangle}_N \check{1} \tag{2.76}$$

$$\simeq \frac{1}{2} \frac{N}{|V|} \left(1 - \frac{N}{|V|} \right). \tag{2.77}$$

31

2.B Some detailed calculations

2.B.1 Proofs of Eqs. (2.26) and (2.27)

We show that the linear transformation given by Eqs. (2.22), (2.23), (2.24), and (2.25) give a canonical transformation, which preserves the canonical commutation relations (2.26) and (2.27). To this end, we assume

$$\left[\hat{\boldsymbol{Q}}_0 \overset{\otimes}{,} \hat{\boldsymbol{P}}_0\right] = i\hbar\check{\mathbb{1}}, \tag{2.78}$$

$$\left[\hat{\boldsymbol{q}}_n \overset{\otimes}{,} \hat{\boldsymbol{p}}_m\right] = i\hbar\delta_{m,n}\check{\mathbb{1}}, \tag{2.79}$$

$$\left[\hat{\boldsymbol{Q}}_0 \overset{\otimes}{,} \hat{\boldsymbol{p}}_n\right] = 0, \tag{2.80}$$

$$\left[\hat{\boldsymbol{q}}_n \overset{\otimes}{,} \hat{\boldsymbol{P}}_0\right] = 0. \tag{2.81}$$

Evaluating the commutation relations for the variables $\hat{\mathcal{Q}}$, $\hat{\mathcal{P}}$, $\{\hat{r}_n\}_{n=1}^N$, and $\{\hat{\pi}_n\}_{n=1}^N$, we have

$$\left[\hat{\mathcal{Q}} \overset{\otimes}{,} \hat{\mathcal{P}}\right] = \left[\frac{\hat{Q}_0 + \mu \sum_{m=1}^N \hat{q}_m}{1 + N\mu} \overset{\otimes}{,} \hat{P}_0 + \sum_{n=1}^N \hat{p}_n\right] \tag{2.82}$$

$$= \frac{1}{1 + N\mu}\left(\underbrace{\left[\hat{Q}_0 \overset{\otimes}{,} \hat{P}_0\right]}_{i\hbar\check{I}} + \mu \sum_{m=1}^N \sum_{n=1}^N \underbrace{\left[\hat{q}_m \overset{\otimes}{,} \hat{p}_n\right]}_{i\hbar\delta_{m,n}\check{I}}\right) \tag{2.83}$$

$$= i\hbar\check{I}, \tag{2.84}$$

$$\left[\hat{r}_n \overset{\otimes}{,} \hat{\pi}_m\right] = \left[\hat{q}_n - \frac{\hat{Q}_0 + \mu \sum_{l=1}^N \hat{q}_l}{1 + N\mu} \overset{\otimes}{,} \hat{p}_m - \mu\hat{P}_0\right] \tag{2.85}$$

$$= \left[\hat{q}_n - \frac{\mu}{1 + N\mu}\sum_{l=1}^N \hat{q}_l \overset{\otimes}{,} \hat{p}_m\right] + \frac{\mu}{1 + N\mu}\left[\hat{Q}_0 \overset{\otimes}{,} \hat{P}_0\right] \tag{2.86}$$

$$= \underbrace{\left[\hat{q}_n \overset{\otimes}{,} \hat{p}_m\right]}_{i\hbar\delta_{n,m}\check{I}} - \frac{\mu}{1 + N\mu}\sum_{l=1}^N \underbrace{\left[\hat{q}_l \overset{\otimes}{,} \hat{p}_m\right]}_{i\hbar\delta_{l,m}\check{I}} + \frac{\mu}{1 + N\mu}\underbrace{\left[\hat{Q}_0 \overset{\otimes}{,} \hat{P}_0\right]}_{i\hbar\check{I}} \tag{2.87}$$

$$= i\hbar\delta_{n,m}\check{I}, \tag{2.88}$$

$$\left[\hat{\mathcal{Q}} \overset{\otimes}{,} \hat{\pi}_n\right] = \left[\frac{\hat{Q}_0 + \mu \sum_{m=1}^N \hat{q}_m}{1 + N\mu} \overset{\otimes}{,} \hat{p}_n - \mu\hat{P}_0\right] \tag{2.89}$$

$$= -\frac{\mu}{1 + N\mu}\underbrace{\left[\hat{Q}_0 \overset{\otimes}{,} \hat{P}_0\right]}_{i\hbar\check{I}} + \frac{\mu}{1 + N\mu}\sum_{m=1}^N \underbrace{\left[\hat{q}_m \overset{\otimes}{,} \hat{p}_n\right]}_{i\hbar\delta_{m,n}\check{I}} \tag{2.90}$$

$$= 0, \tag{2.91}$$

$$\left[\hat{r}_n \overset{\otimes}{,} \hat{P}_0\right] = \left[\hat{q}_n - \frac{\hat{Q}_0 + \mu \sum_{m=1}^N \hat{q}_m}{1 + N\mu} \overset{\otimes}{,} \hat{P}_0 + \sum_{l=1}^N \hat{p}_l\right] \tag{2.92}$$

$$= \sum_{l=1}^N \underbrace{\left[\hat{q}_n \overset{\otimes}{,} \hat{p}_l\right]}_{=i\hbar\delta_{n,l}\check{I}} - \frac{\mu}{1 + N\mu}\sum_{m=1}^N \sum_{l=1}^N \underbrace{\left[\hat{q}_m \overset{\otimes}{,} \hat{p}_l\right]}_{=i\hbar\delta_{m,l}\check{I}} - \frac{1}{1 + N\mu}\underbrace{\left[\hat{Q}_0 \overset{\otimes}{,} \hat{P}_0\right]}_{i\hbar\check{I}} \tag{2.93}$$

$$= 0, \tag{2.94}$$

33

which proves Eqs. (2.26) and (2.27).

2.B.2   Proof of Eq. (2.28)

We invert the definitions

$$\hat{\mathcal{Q}} := \frac{\hat{Q}_0 + \mu \sum_{n=1}^{N} \hat{q}_n}{1 + N\mu}, \tag{2.22}$$

$$\hat{r}_n := \hat{q}_n - \frac{\hat{Q}_0 + \mu \sum_{n=1}^{N} \hat{q}_n}{1 + N\mu} \quad (n = 1, 2, \ldots, N), \tag{2.23}$$

$$\hat{\mathcal{P}} := \hat{P}_0 + \sum_{n=1}^{N} \hat{p}_n, \tag{2.24}$$

$$\hat{\pi}_n := \hat{p}_n - \mu \hat{P}_0 \quad (n = 1, 2, \ldots, N). \tag{2.25}$$

and put the expressions

$$\hat{Q}_0 = \hat{\mathcal{Q}} - N\mu \hat{R}_{\mathrm{B}}, \tag{2.95}$$

$$\hat{q}_n = \hat{\mathcal{Q}} + \hat{r}_n \quad (n = 1, 2, \ldots, N) \tag{2.96}$$

$$\hat{P}_0 = \frac{1}{1 + N\mu} \left(\hat{\mathcal{P}} - \hat{\Pi}_{\mathrm{B}} \right), \tag{2.97}$$

$$\hat{p}_n = \hat{\pi}_n + \frac{\mu}{1 + N\mu} \left(\hat{\mathcal{P}} - \hat{\Pi}_{\mathrm{B}} \right) \quad (n = 1, 2, \ldots, N) \tag{2.98}$$

directly into the total Hamiltonian (2.11). We then obtain

$$\hat{\mathcal{H}}_0 = \frac{1}{2M_0}\left(\frac{1}{1+N\mu}\right)^2\left(\hat{\mathcal{P}}-\hat{\mathbf{\Pi}}_{\mathrm{B}}\right)^2 + V_0(\hat{\mathcal{Q}}-N\mu\hat{\mathbf{R}}_{\mathrm{B}}) \tag{2.99}$$

$$= \underbrace{\frac{1}{2\mathcal{M}_{\mathrm{tot}}}\frac{1}{1+N\mu}\left(\hat{\mathcal{P}}-\hat{\mathbf{\Pi}}_{\mathrm{B}}\right)^2}_{=:\hat{K}_0} + V_0(\hat{\mathcal{Q}}-N\mu\hat{\mathbf{R}}_{\mathrm{B}}), \tag{2.100}$$

$$\hat{\mathcal{H}}_{\mathrm{IB}}[\hat{\mathbf{Q}}_0] = \sum_{n=1}^{N}\left\{\frac{1}{2m_{\mathrm{B}}}\left[\hat{\boldsymbol{\pi}}_n + \frac{\mu}{1+N\mu}\left(\hat{\mathcal{P}}-\hat{\mathbf{\Pi}}_{\mathrm{B}}\right)\right]^2 + V_{\mathrm{B}}(\hat{\boldsymbol{r}}_n + N\mu\hat{\mathbf{R}}_{\mathrm{B}})\right\}$$
$$+ \frac{g}{2}\sum_{n\neq m}\delta(\hat{\boldsymbol{r}}_n - \hat{\boldsymbol{r}}_m) \tag{2.101}$$

$$= \underbrace{\frac{1}{\mathcal{M}_{\mathrm{tot}}}\hat{\mathbf{\Pi}}_{\mathrm{B}}\cdot\left(\hat{\mathcal{P}}-\hat{\mathbf{\Pi}}_{\mathrm{B}}\right) + \frac{1}{2\mathcal{M}_{\mathrm{tot}}}\frac{N\mu}{1+N\mu}\left(\hat{\mathcal{P}}-\hat{\mathbf{\Pi}}_{\mathrm{B}}\right)^2}_{=:\hat{K}_1}$$

$$+ \sum_{n=1}^{N}\left[\frac{\hat{\boldsymbol{\pi}}_n^2}{2m_{\mathrm{B}}} + V_{\mathrm{B}}(\hat{\boldsymbol{r}}_n + N\mu\hat{\mathbf{R}}_{\mathrm{B}})\right] + \frac{g}{2}\sum_{n\neq m}\delta(\hat{\boldsymbol{r}}_n - \hat{\boldsymbol{r}}_m). \tag{2.102}$$

Gathering the terms $\hat{K}_0$ and $\hat{K}_1$ into

$$\hat{K}_0 + \hat{K}_1 = \underbrace{\left[\frac{1}{2\mathcal{M}_{\mathrm{tot}}}\frac{1}{1+N\mu} + \frac{1}{2\mathcal{M}_{\mathrm{tot}}}\frac{N\mu}{1+N\mu}\right]}_{=1/(2\mathcal{M}_{\mathrm{tot}})}\left(\hat{\mathcal{P}}-\hat{\mathbf{\Pi}}_{\mathrm{B}}\right)^2$$

$$+ \frac{1}{\mathcal{M}_{\mathrm{tot}}}\hat{\mathbf{\Pi}}_{\mathrm{B}}\cdot\left(\hat{\mathcal{P}}-\hat{\mathbf{\Pi}}_{\mathrm{B}}\right) \tag{2.103}$$

$$= \frac{1}{2\mathcal{M}_{\mathrm{tot}}}\underbrace{\left[(\hat{\mathcal{P}}-\hat{\mathbf{\Pi}}_{\mathrm{B}})^2 + 2\hat{\mathbf{\Pi}}_{\mathrm{B}}\cdot(\hat{\mathcal{P}}-\hat{\mathbf{\Pi}}_{\mathrm{B}})\right]}_{\hat{\mathcal{P}}^2-\hat{\mathbf{\Pi}}_{\mathrm{B}}^2} \tag{2.104}$$

$$= \frac{\hat{\mathcal{P}}^2}{2\mathcal{M}_{\mathrm{tot}}} - \frac{\hat{\mathbf{\Pi}}_{\mathrm{B}}^2}{2\mathcal{M}_{\mathrm{tot}}}, \tag{2.105}$$

35

we finally arrive at

$$\hat{\mathcal{H}}_{\text{tot}} = \hat{\mathcal{H}}_0 + \hat{\mathcal{H}}_{\text{IB}}[\hat{\pmb{Q}}_0] \tag{2.106}$$

$$= \frac{\hat{\pmb{\mathcal{P}}}^2}{2\mathcal{M}_{\text{tot}}} - \frac{\hat{\pmb{\Pi}}_{\text{B}}^2}{2\mathcal{M}_{\text{tot}}} + V_0(\hat{\pmb{\mathcal{Q}}} - N\mu\hat{\pmb{R}}_{\text{B}})$$
$$+ \sum_{n=1}^{N}\left[\frac{\hat{\pmb{\pi}}_n^2}{2m_{\text{B}}} + V_{\text{B}}(\hat{\pmb{r}}_n + N\mu\hat{\pmb{R}}_{\text{B}})\right] + \frac{g}{2}\sum_{n\neq m}\delta(\hat{\pmb{r}}_n - \hat{\pmb{r}}_m). \tag{2.107}$$

2.B.3 Derivation of formulas (2.33), (2.34), (2.35), and (2.36)

First, we show the formulas

$$\hat{U}_N\hat{\pmb{r}}_n\hat{U}_N^{\dagger} = \hat{\pmb{r}}_n - \frac{N\mu}{1+N\mu}\hat{\pmb{R}}_{\text{B}}, \tag{2.33}$$

$$\hat{U}_N\hat{\pmb{\pi}}_n\hat{U}_N^{\dagger} = \hat{\pmb{\pi}}_n + \mu\hat{\pmb{\Pi}}_{\text{B}}, \tag{2.34}$$

using the general expression

$$e^{\hat{A}}\hat{B}e^{-\hat{A}} = \sum_{k=0}^{\infty}\frac{1}{k!}\text{ad}_{\hat{A}}^k\hat{B} \tag{2.108}$$

for a set of arbitrary operators $\hat{A}$ and $\hat{B}$. Here, we introduced the notation

$$\text{ad}_{\hat{A}}^k\hat{B} := \underbrace{[\hat{A},[\hat{A},[\cdots[\hat{A},\hat{B}]]]]}_{k} \tag{2.109}$$

for the adjoint operation. The remaining formulas

$$\hat{U}_N\hat{\pmb{R}}_{\text{B}}\hat{U}_N^{\dagger} = \frac{1}{1+N\mu}\hat{\pmb{R}}_{\text{B}}, \tag{2.35}$$

$$\hat{U}_N\hat{\pmb{\Pi}}_{\text{B}}\hat{U}_N^{\dagger} = (1+N\mu)\hat{\pmb{\Pi}}_{\text{B}} \tag{2.36}$$

immediately follow Eqs. (2.33) and (2.34), respectively.

To show Eq. (2.33), we put

$$\hat{A} = \frac{c_N}{2i\hbar}\left(\hat{\pmb{R}}_{\text{B}}\cdot\hat{\pmb{\Pi}}_{\text{B}} + \hat{\pmb{\Pi}}_{\text{B}}\cdot\hat{\pmb{R}}_{\text{B}}\right), \quad \hat{B} = \hat{\pmb{r}}_n \tag{2.110}$$

and evaluate the right-hand side of Eq. (2.108). In this case, we can show that

$$\left(\mathrm{ad}_{\hat{A}}^{k}\hat{B}\right)_{\text{Eq. (2.110)}} = \begin{cases} \hat{\boldsymbol{r}}_{n}, & (k = 0) \\ (-c_N)^k \hat{\boldsymbol{R}}_{\mathrm{B}}, & (k \geq 1) \end{cases} \tag{2.111}$$

and consequently have

$$\hat{U}_N \hat{\boldsymbol{r}}_n \hat{U}_N^{\dagger} = \sum_{k=0}^{\infty} \frac{1}{k!} \left(\mathrm{ad}_{\hat{A}}^{k}\hat{B}\right)_{\text{Eq. (2.110)}} \tag{2.112}$$

$$= \hat{\boldsymbol{r}}_n + \sum_{k=1}^{\infty} \frac{(-c_N)^k}{k!} \hat{\boldsymbol{R}}_{\mathrm{B}} \tag{2.113}$$

$$= \hat{\boldsymbol{r}}_n + \left(\mathrm{e}^{-c_N} - 1\right) \hat{\boldsymbol{R}}_{\mathrm{B}} \tag{2.114}$$

$$= \hat{\boldsymbol{r}}_n + \left(\frac{1}{1 + N\mu} - 1\right) \hat{\boldsymbol{R}}_{\mathrm{B}} \tag{2.115}$$

$$= \hat{\boldsymbol{r}}_n - \frac{N\mu}{1 + N\mu} \hat{\boldsymbol{R}}_{\mathrm{B}}. \tag{2.116}$$

We can prove Eq. (2.111) by mathematical induction. The case of $k = 0$ trivially holds. For the case of $k = 1$, it holds that

$$\left(\mathrm{ad}_{\hat{A}}^{1}\hat{B}\right)_{\text{Eq. (2.110)}} = \frac{c_N}{2i\hbar} \left[\hat{\boldsymbol{R}}_{\mathrm{B}} \cdot \hat{\boldsymbol{\Pi}}_{\mathrm{B}} + \hat{\boldsymbol{\Pi}}_{\mathrm{B}} \cdot \hat{\boldsymbol{R}}_{\mathrm{B}}, \hat{\boldsymbol{r}}_n\right] \tag{2.117}$$

$$= \frac{c_N}{2i\hbar} \sum_{m=1}^{N} \left[\hat{\boldsymbol{R}}_{\mathrm{B}} \cdot \hat{\boldsymbol{\pi}}_m + \hat{\boldsymbol{\pi}}_m \cdot \hat{\boldsymbol{R}}_{\mathrm{B}}, \hat{\boldsymbol{r}}_n\right] \tag{2.118}$$

$$= \frac{c_N}{2i\hbar} \sum_{m=1}^{N} \left(\hat{\boldsymbol{R}}_{\mathrm{B}} \circ \underbrace{\left[\hat{\boldsymbol{\pi}}_m \overset{\otimes}{,} \hat{\boldsymbol{r}}_n\right]}_{= -i\hbar \delta_{m,n} \check{\mathrm{I}}} + \underbrace{\left[\hat{\boldsymbol{\pi}}_m \overset{\otimes}{,} \hat{\boldsymbol{r}}_n\right]}_{= -i\hbar \delta_{m,n} \check{\mathrm{I}}} \circ \hat{\boldsymbol{R}}_{\mathrm{B}}\right) \tag{2.119}$$

$$= -c_N \hat{\boldsymbol{R}}_{\mathrm{B}}. \tag{2.120}$$

Here, assuming that

$$\left(\mathrm{ad}_{\hat{A}}^{k}\hat{B}\right)_{\text{Eq. (2.110)}} = (-c_N)^k \hat{\boldsymbol{R}}_{\mathrm{B}} \tag{2.121}$$

for an integer $k \geq 2$, we have

$$\left(\text{ad}_{\hat{A}}^{k+1}\hat{B}\right)_{\text{Eq. (2.110)}} = \frac{c_N}{2i\hbar}\left[\hat{R}_\text{B} \cdot \hat{\Pi}_\text{B} + \hat{\Pi}_\text{B} \cdot \hat{R}_\text{B}, \left(\text{ad}_{\hat{A}}^{k}\hat{B}\right)_{\text{Eq. (2.110)}}\right] \quad (2.122)$$

$$= -\frac{(-c_N)^{k+1}}{2i\hbar}[\hat{R}_\text{B} \cdot \hat{\Pi}_\text{B} + \hat{\Pi}_\text{B} \cdot \hat{R}_\text{B}, \hat{R}_\text{B}] \quad (2.123)$$

$$= (-c_N)^{k+1}\hat{R}_\text{B}. \quad (2.124)$$

Here, we used the fact

$$[\hat{R}_\text{B} \cdot \hat{\Pi}_\text{B} + \hat{\Pi}_\text{B} \cdot \hat{R}_\text{B}, \hat{R}_\text{B}] = \hat{R}_\text{B} \circ \underbrace{\left[\hat{\Pi}_\text{B} \overset{\otimes}{,} \hat{R}_\text{B}\right]}_{=-i\hbar\breve{I}} + \underbrace{\left[\hat{\Pi}_\text{B} \overset{\otimes}{,} \hat{R}_\text{B}\right]}_{=-i\hbar\breve{I}} \circ \hat{R}_\text{B} \quad (2.125)$$

$$= -2i\hbar\hat{R}_\text{B}. \quad (2.126)$$

Equation (2.111) is thus proven by induction.

To show Eq. (2.128), we similarly put

$$\hat{A} = \frac{c_N}{2i\hbar}\left(\hat{R}_\text{B} \cdot \hat{\Pi}_\text{B} + \hat{\Pi}_\text{B} \cdot \hat{R}_\text{B}\right), \quad \hat{B} = \hat{\pi}_n \quad (2.127)$$

in Eq. (2.108). In this case, we can show that

$$\left(\text{ad}_{\hat{A}}^{k}\hat{B}\right)_{\text{Eq. (2.127)}} = \begin{cases} \hat{\pi}_n & (k = 0) \\ c_N^k\hat{\Pi}_\text{B}/N & (k \geq 1) \end{cases}, \quad (2.128)$$

and consequently have

$$\hat{U}_N\hat{\pi}_n\hat{U}_N^\dagger = \sum_{k=0}^{\infty}\frac{1}{k!}\left(\text{ad}_{\hat{A}}^{k}\hat{B}\right)_{\text{Eq. (2.127)}} \quad (2.129)$$

$$= \hat{\pi}_n + \sum_{k=1}^{\infty}\frac{1}{k!}\frac{c_N^k}{N}\hat{\Pi}_\text{B} \quad (2.130)$$

$$= \hat{\pi}_n + \frac{1}{N}\left(e^{c_N} - 1\right)\hat{\Pi}_\text{B} \quad (2.131)$$

$$= \hat{\pi}_n + \mu\hat{\Pi}_\text{B}. \quad (2.132)$$

In Eq. (2.128), the case of $k = 0$ trivially holds. For the case of $k = 1$, it holds that

$$\left(\mathrm{ad}_{\hat{A}}^1 \hat{B}\right)_{\text{Eq. (2.127)}} = \frac{c_N}{2i\hbar}\left[\hat{\boldsymbol{R}}_{\text{B}} \cdot \hat{\boldsymbol{\Pi}}_{\text{B}} + \hat{\boldsymbol{\Pi}}_{\text{B}} \cdot \hat{\boldsymbol{R}}_{\text{B}}, \hat{\boldsymbol{\pi}}_n\right] \tag{2.133}$$

$$= \frac{c_N}{2i\hbar}\frac{1}{N}\sum_{m=1}^{N}\left[\hat{\boldsymbol{r}}_m \cdot \hat{\boldsymbol{\Pi}}_{\text{B}} + \hat{\boldsymbol{\Pi}}_{\text{B}} \cdot \hat{\boldsymbol{r}}_m, \hat{\boldsymbol{\pi}}_n\right] \tag{2.134}$$

$$= \frac{c_N}{2i\hbar}\frac{1}{N}\sum_{m=1}^{N}\left(\underbrace{\left[\hat{\boldsymbol{r}}_n \overset{\otimes}{\text{,}} \hat{\boldsymbol{\pi}}_n\right]}_{=i\hbar\delta_{m,n}\check{\boldsymbol{1}}}\circ\hat{\boldsymbol{\Pi}}_{\text{B}} + \hat{\boldsymbol{\Pi}}_{\text{B}}\circ\underbrace{\left[\hat{\boldsymbol{r}}_n \overset{\otimes}{\text{,}} \hat{\boldsymbol{\pi}}_n\right]}_{=i\hbar\delta_{m,n}\check{\boldsymbol{1}}}\right) \tag{2.135}$$

$$= \frac{c_N}{N}\hat{\boldsymbol{\Pi}}_{\text{B}}. \tag{2.136}$$

Here, assuming that

$$\left(\mathrm{ad}_{\hat{A}}^k \hat{B}\right)_{\text{Eq. (2.127)}} = \frac{c_N^k}{N}\hat{\boldsymbol{\Pi}}_{\text{B}} \tag{2.137}$$

for an integer $k \geq 2$, we have

$$\left(\mathrm{ad}_{\hat{A}}^{k+1} \hat{B}\right)_{\text{Eq. (2.127)}} = \frac{c_N}{2i\hbar}\left[\hat{\boldsymbol{R}}_{\text{B}} \cdot \hat{\boldsymbol{\Pi}}_{\text{B}} + \hat{\boldsymbol{\Pi}}_{\text{B}} \cdot \hat{\boldsymbol{R}}_{\text{B}}, \left(\mathrm{ad}_{\hat{A}}^k \hat{B}\right)_{\text{Eq. (2.127)}}\right] \tag{2.138}$$

$$= \frac{1}{N}\frac{c_N^{k+1}}{2i\hbar}[\hat{\boldsymbol{R}}_{\text{B}} \cdot \hat{\boldsymbol{\Pi}}_{\text{B}} + \hat{\boldsymbol{\Pi}}_{\text{B}} \cdot \hat{\boldsymbol{R}}_{\text{B}}, \hat{\boldsymbol{\Pi}}_{\text{B}}] \tag{2.139}$$

$$= \frac{c_N^{k+1}}{N}\hat{\boldsymbol{\Pi}}_{\text{B}}. \tag{2.140}$$

Here, we used the fact

$$[\hat{\boldsymbol{R}}_{\text{B}} \cdot \hat{\boldsymbol{\Pi}}_{\text{B}} + \hat{\boldsymbol{\Pi}}_{\text{B}} \cdot \hat{\boldsymbol{R}}_{\text{B}}, \hat{\boldsymbol{\Pi}}_{\text{B}}] = \underbrace{\left[\hat{\boldsymbol{R}}_{\text{B}} \overset{\otimes}{\text{,}} \hat{\boldsymbol{\Pi}}_{\text{B}}\right]}_{=i\hbar\check{\boldsymbol{1}}}\circ\hat{\boldsymbol{\Pi}}_{\text{B}} + \hat{\boldsymbol{\Pi}}_{\text{B}}\circ\underbrace{\left[\hat{\boldsymbol{R}}_{\text{B}} \overset{\otimes}{\text{,}} \hat{\boldsymbol{\Pi}}_{\text{B}}\right]}_{=i\hbar\check{\boldsymbol{1}}} \tag{2.141}$$

$$= 2i\hbar\hat{\boldsymbol{\Pi}}_{\text{B}}. \tag{2.142}$$

Eq. (2.111) is thus proven by induction.

39

2.B.4 Derivation of Eq. (2.37)

We put the equations

$$\hat{U}_N \hat{r}_n \hat{U}_N^\dagger = \hat{r}_n - \frac{N\mu}{1+N\mu}\hat{R}_B, \tag{2.33}$$

$$\hat{U}_N \hat{\pi}_n \hat{U}_N^\dagger = \hat{\pi}_n + \mu\hat{\Pi}_B, \tag{2.34}$$

$$\hat{U}_N \hat{R}_B \hat{U}_N^\dagger = \frac{1}{1+N\mu}\hat{R}_B, \tag{2.35}$$

$$\hat{U}_N \hat{\Pi}_B \hat{U}_N^\dagger = (1+N\mu)\hat{\Pi}_B, \tag{2.36}$$

directly into the expression

$$\hat{\mathcal{H}}_{\text{tot}} = \frac{\hat{\mathcal{P}}^2}{2\mathcal{M}_{\text{tot}}} - \frac{\hat{\Pi}_B^2}{2\mathcal{M}_{\text{tot}}} + V_0(\hat{\mathcal{Q}} - N\mu\hat{R}_B)$$
$$+ \sum_{n=1}^{N}\left[\frac{\hat{\pi}_n^2}{2m_B} + V_B(\hat{r}_n + N\mu\hat{R}_B)\right] + \frac{g}{2}\sum_{n\neq m}\delta(\hat{r}_n - \hat{r}_m) \tag{2.28}$$

to show that

$$\hat{U}_N \hat{\mathcal{H}}_{\text{tot}} \hat{U}_N^\dagger = \frac{\hat{\mathcal{P}}^2}{2\mathcal{M}_{\text{tot}}} + \frac{\hat{\Pi}_B^2}{2M_0} + V_0(\hat{\mathcal{Q}} - \gamma_N\hat{R}_B)$$
$$+ \sum_{n=1}^{N}\left[\frac{\hat{\pi}_n^2}{2m_B} + V_B(\hat{r}_n)\right] + \frac{g}{2}\sum_{n\neq m}\delta(\hat{r}_n - \hat{r}_m). \tag{2.37}$$

First, the $\{\hat{r}_n\}$-dependent terms in Eq. (2.28) are transformed as

$$\hat{U}_N\left[V_0(\hat{\mathcal{Q}} - N\mu\hat{R}_B) + \sum_{n=1}^{N}V_B(\hat{r}_n + N\mu\hat{R}_B) + \frac{g}{2}\sum_{n\neq m}\delta(\hat{r}_n - \hat{r}_m)\right]\hat{U}_N^\dagger \tag{2.143}$$

$$= V_0(\hat{\mathcal{Q}} - \tilde{\gamma}_N\hat{R}_B) + \sum_{n=1}^{N}V_B(\hat{r}_n) + \frac{g}{2}\sum_{n\neq m}\delta(\hat{r}_n - \hat{r}_m), \tag{2.144}$$

where $\tilde{\gamma}_N := N\mu/(1+N\mu)$. Second, the remaining $\{\hat{\pi}_n\}$-dependent terms are transformed as

$$\hat{U}_N\left[-\frac{\hat{\Pi}_B^2}{2\mathcal{M}_{\text{tot}}} + \sum_{n=1}^{N}\frac{\hat{\pi}_n^2}{2m_B}\right]\hat{U}_N^\dagger = \frac{\hat{\Pi}_B^2}{2M_0} + \sum_{n=1}^{N}\frac{\hat{\pi}_n^2}{2m_B}. \tag{2.145}$$

We then have Eq. (2.37). Here, Eq. (2.145) is derived from

$$\hat{U}_N \left(-\frac{\hat{\boldsymbol{\Pi}}_{\mathrm{B}}^2}{2\mathcal{M}_{\mathrm{tot}}} \right) \hat{U}_N^\dagger = -\frac{1}{2\mathcal{M}_{\mathrm{tot}}} \left(\hat{U}_N \hat{\boldsymbol{\Pi}}_{\mathrm{B}} \hat{U}_N \right)^2 \tag{2.146}$$

$$= -\frac{1}{2\mathcal{M}_{\mathrm{tot}}} (1 + N\mu)^2 \hat{\boldsymbol{\Pi}}_{\mathrm{B}}^2 \tag{2.147}$$

$$= -\frac{1}{2M_0} (1 + N\mu) \hat{\boldsymbol{\Pi}}_{\mathrm{B}}^2, \tag{2.148}$$

$$\hat{U}_N \left(\sum_{n=1}^N \frac{\hat{\boldsymbol{\pi}}_n^2}{2m_{\mathrm{B}}} \right) \hat{U}_N^\dagger = \frac{1}{2m_{\mathrm{B}}} \sum_{n=1}^N \left(\hat{U}_N \hat{\boldsymbol{\pi}}_n \hat{U}_N^\dagger \right)^2 \tag{2.149}$$

$$= \frac{1}{2m_{\mathrm{B}}} \sum_{n=1}^N \left(\hat{\boldsymbol{\pi}}_n + \mu \hat{\boldsymbol{\Pi}}_{\mathrm{B}} \right)^2 \tag{2.150}$$

$$= \frac{1}{2m_{\mathrm{B}}} \sum_{n=1}^N \hat{\boldsymbol{\pi}}_n^2 + \frac{1}{2M_0} (2 + N\mu) \hat{\boldsymbol{\Pi}}_{\mathrm{B}}^2. \tag{2.151}$$

2.C Indistinguishability of identical particles

We show that symmetrizing the Hamiltonian (2.11) with repsect to the variables $\{\hat{\boldsymbol{q}}_n\}_{n=1}^N$ also means that for the variables $\{\hat{\boldsymbol{r}}_n\}_{n=1}^N$. To this end, we express the linear transformation given by Eqs. (2.22), (2.23), (2.24), and (2.25) in the

matrix notation:

$$
\begin{bmatrix} \hat{\mathcal{Q}} \\ \hat{\boldsymbol{r}}_1 \\ \vdots \\ \hat{\boldsymbol{r}}_N \end{bmatrix} = \underbrace{\begin{bmatrix} A_{0,0} & A_{0,1} & \cdots & A_{0,N} \\ A_{1,0} & A_{1,1} & \cdots & A_{1,N} \\ \vdots & \vdots & \ddots & \vdots \\ A_{N,0} & A_{N,1} & \cdots & A_{N,N} \end{bmatrix}}_{=:A} \begin{bmatrix} \hat{\boldsymbol{Q}}_0 \\ \hat{\boldsymbol{q}}_1 \\ \vdots \\ \hat{\boldsymbol{q}}_N \end{bmatrix} ,
\tag{2.152}
$$

$$
\begin{bmatrix} \hat{\mathcal{P}} \\ \hat{\boldsymbol{\pi}}_1 \\ \vdots \\ \hat{\boldsymbol{\pi}}_N \end{bmatrix} = \underbrace{\begin{bmatrix} B_{0,0} & B_{0,1} & \cdots & B_{0,N} \\ B_{1,0} & B_{1,1} & \cdots & B_{1,N} \\ \vdots & \vdots & \ddots & \vdots \\ B_{N,0} & B_{N,1} & \cdots & B_{N,N} \end{bmatrix}}_{=:B} \begin{bmatrix} \hat{\boldsymbol{P}}_0 \\ \hat{\boldsymbol{p}}_1 \\ \vdots \\ \hat{\boldsymbol{p}}_N \end{bmatrix}
\tag{2.153}
$$

We then take the basis

$$
\left| \boldsymbol{Q}_0, \ldots, \boldsymbol{q}_N \right\rangle := \left| \boldsymbol{Q}_0 \right\rangle \otimes \frac{1}{\sqrt{N!}} \left[\prod_{n=1}^{N} \hat{\psi}^\dagger(\boldsymbol{q}_n) \right] \left| 0 \right\rangle ,
\tag{2.154}
$$

which is symmetrized with respect to any variables. Here, the field operator $\hat{\psi}^\dagger(\boldsymbol{q})$ satisfies the condition

$$
[\hat{\psi}(\boldsymbol{q}), \hat{\psi}^\dagger(\boldsymbol{q}')] = i\hbar\delta(\boldsymbol{q} - \boldsymbol{q}'),
\tag{2.155}
$$

$$
[\hat{\psi}(\boldsymbol{q}), \hat{\psi}(\boldsymbol{q}')] = [\hat{\psi}^\dagger(\boldsymbol{q}), \hat{\psi}^\dagger(\boldsymbol{q}')] = 0.
\tag{2.156}
$$

The dynamical variables $\{(\hat{\boldsymbol{q}}_n, \hat{\boldsymbol{p}}_n)\}_{n=1}^{N}$ are also expressed as

$$
\hat{\boldsymbol{q}}_n = \int d\boldsymbol{Q}_0 d\boldsymbol{q}_1 \cdots d\boldsymbol{q}_N \left| \boldsymbol{Q}_0, \ldots, \boldsymbol{q}_N \right\rangle \boldsymbol{q}_n \left\langle \boldsymbol{Q}_0, \ldots, \boldsymbol{q}_N \right| ,
\tag{2.157}
$$

$$
\hat{\boldsymbol{p}}_n = \int d\boldsymbol{Q}_0 d\boldsymbol{q}_1 \cdots d\boldsymbol{q}_N \left| \boldsymbol{Q}_0, \ldots, \boldsymbol{q}_N \right\rangle (-i\hbar\nabla_n) \left\langle \boldsymbol{Q}_0, \ldots, \boldsymbol{q}_N \right| .
\tag{2.158}
$$

First, we can show that

$$\hat{r}_n = \frac{1}{\det[A]} \int d\boldsymbol{Q}_0 d\boldsymbol{q}_1 \cdots d\boldsymbol{q}_N$$

$$\times |A^{-1}\boldsymbol{Q}_0,\ldots,A^{-1}\boldsymbol{q}_N\rangle \boldsymbol{q}_n \langle A^{-1}\boldsymbol{Q}_0,\ldots,A^{-1}\boldsymbol{q}_N|, \qquad (2.159)$$

$$\hat{\pi}_n = \frac{1}{\det[A]} \int d\boldsymbol{Q}_0 d\boldsymbol{q}_1 \cdots d\boldsymbol{q}_N$$

$$\times |A^{-1}\boldsymbol{Q}_0,\ldots,A^{-1}\boldsymbol{q}_N\rangle (-i\hbar\nabla_n) \langle A^{-1}\boldsymbol{Q}_0,\ldots,A^{-1}\boldsymbol{q}_N|; \qquad (2.160)$$

see also a later paragraph (**Proof of Eqs.** (2.159) **and** (2.160)). This means that taking the variables $\{\hat{r}_n\}_{n=1}^N$ instead of $\{\hat{q}_n\}_{n=1}^N$ effectively replaces the basis $\left|\boldsymbol{Q}_0,\ldots,\boldsymbol{q}_N\right\rangle$ by $|A^{-1}\boldsymbol{Q}_0,\ldots,A^{-1}\boldsymbol{q}_N\rangle$. These bases have generally different exchange symmetries:

$$|\boldsymbol{Q}_0,\ldots,\underline{\boldsymbol{q}_k},\ldots,\underline{\boldsymbol{q}_l},\ldots,\boldsymbol{q}_N\rangle \qquad (2.161)$$

$$= |\boldsymbol{Q}_0,\ldots,\underline{\boldsymbol{q}_l},\ldots,\underline{\boldsymbol{q}_k},\ldots,\boldsymbol{q}_N\rangle, \quad (1 \le k < l \le N) \qquad (2.162)$$

$$|A^{-1}\boldsymbol{Q}_0,\ldots,\underline{A^{-1}\boldsymbol{q}_k},\ldots,\underline{A^{-1}\boldsymbol{q}_l},\ldots,A^{-1}\boldsymbol{q}_N\rangle \qquad (2.163)$$

$$= |A^{-1}\boldsymbol{Q}_0,\ldots,\underline{A^{-1}\boldsymbol{q}_l},\ldots,\underline{A^{-1}\boldsymbol{q}_k},\ldots,A^{-1}\boldsymbol{q}_N\rangle. \quad (1 \le k < l \le N) \qquad (2.164)$$

Here, we show that these symmetries are actually equivalent. Indeed, it holds

that

$$\left[A^{-1}Q_0\right]_{q_k \leftrightarrow q_l} = \underbrace{\left[A^{-1}\right]_{k',0}}_{=1} Q_0 + \sum_{m \neq k,l}^{N} \underbrace{\left[A^{-1}\right]_{k',m}}_{=-\mu} q_m$$

$$+ \underbrace{\left[A^{-1}\right]_{k',k}}_{=-\mu} q_l + \underbrace{\left[A^{-1}\right]_{k',l}}_{=-\mu} q_k \tag{2.165}$$

$$= Q_0 - N\mu\hat{R}_B = \left[A^{-1}Q_0\right]_{(A^{-1}q_k) \leftrightarrow (A^{-1}q_l)}, \tag{2.166}$$

$$\left[A^{-1}q_{k'}\right]_{q_k \leftrightarrow q_l} = \underbrace{\left[A^{-1}\right]_{k',0}}_{=1} Q_0 + \sum_{m \neq k,l}^{N} \underbrace{\left[A^{-1}\right]_{k',m}}_{=\delta_{k',m}} q_m$$

$$+ \underbrace{\left[A^{-1}\right]_{k',k}}_{=\delta_{k',k}} q_l + \underbrace{\left[A^{-1}\right]_{k',l}}_{=\delta_{k',l}} q_k \tag{2.167}$$

$$= \begin{cases} Q_0 + q_{k'} & (k' \neq k,l) \\ Q_0 + q_l & (k' = k) \\ Q_0 + q_k & (k' = l) \end{cases} = \left[A^{-1}q_{k'}\right]_{(A^{-1}q_k) \leftrightarrow (A^{-1}q_l)}. \tag{2.168}$$

In other words, exchanging the variables q_k and q_l is equivalent to exchanging the variables $A^{-1}q_k$ and $A^{-1}q_l$. From this fact, we can safely perform the second-quantizaton procedure for the Hamiltonian both in the $\{(\hat{q}_n, \hat{p}_n)\}_{n=1}^{N}$-representation and the $\{(\hat{r}_n, \hat{\pi}_n)\}_{n=1}^{N}$-representation.

Proof of Eqs. (2.159) and (2.160)

Suppose that $F(\hat{Q}_0, \ldots, \hat{q}_N)$ is an arbitrary function of the variables $\hat{Q}_0$ and $\{\hat{q}_n\}_{n=1}^{N}$. First, let the state $|Q_0, \ldots, q_N\rangle$ give one of its eigenstates:

$$F(\hat{Q}_0, \ldots, \hat{q}_N)|Q_0, \ldots, q_N\rangle = \bar{F}(Q_0, \ldots, q_N)|Q_0, \ldots, x_N\rangle. \tag{2.169}$$

44

Here $\bar{F}(\boldsymbol{Q}_0,\ldots,\boldsymbol{q}_N)$ is the symmetrized version of $F(\boldsymbol{Q}_0,\ldots,\boldsymbol{q}_N)$ with respect to $\{\boldsymbol{q}_n\}_{n=1}^N$. The matrix element of $F(\hat{\boldsymbol{Q}}_0,\ldots,\hat{\boldsymbol{q}}_N)$ is therefore given by

$$\left\langle \boldsymbol{Q}_0'',\boldsymbol{q}_1'',\ldots,\boldsymbol{q}_N'' \middle| F(\hat{\boldsymbol{Q}}_0,\hat{\boldsymbol{q}}_1,\ldots,\hat{\boldsymbol{q}}_N) \middle| \boldsymbol{Q}_0',\boldsymbol{q}_1',\ldots,\boldsymbol{q}_N' \right\rangle \tag{2.170}$$

$$=\bar{F}(\boldsymbol{Q}_0',\boldsymbol{q}_1',\ldots,\boldsymbol{q}_N')\langle \boldsymbol{Q}_0'',\boldsymbol{q}_1'',\ldots,\boldsymbol{q}_N''|\boldsymbol{Q}_0',\boldsymbol{q}_1',\ldots,\boldsymbol{q}_N'\rangle. \tag{2.171}$$

Second, we can take a unitary representation which satisfies

$$\hat{U}\hat{\boldsymbol{Q}}_0\hat{U}^\dagger = A\hat{\boldsymbol{Q}}_0, \tag{2.172}$$

$$\hat{U}\hat{\boldsymbol{q}}_n\hat{U}^\dagger = A\hat{\boldsymbol{q}}_n; \quad (1 \le n \le N) \tag{2.173}$$

see also a later paragraph (**Unitary representation of linear canonical transformation**). Using the unitary representation and assuming the ansatz solution

$$\hat{U}\left|\boldsymbol{Q}_0,\boldsymbol{q}_1,\ldots,\boldsymbol{q}_N\right\rangle = \mathcal{J}\,|\tilde{\boldsymbol{Q}}_0,\tilde{\boldsymbol{q}}_1,\ldots,\tilde{\boldsymbol{q}}_N\rangle, \tag{2.174}$$

we have

$$\left\langle \boldsymbol{Q}_0'',\boldsymbol{q}_1'',\ldots,\boldsymbol{q}_N'' \middle| F(\hat{\boldsymbol{Q}}_0,\hat{\boldsymbol{q}}_1,\ldots,\hat{\boldsymbol{q}}_N) \middle| \boldsymbol{Q}_0',\boldsymbol{q}_1',\ldots,\boldsymbol{q}_N' \right\rangle \tag{2.175}$$

$$=\left\langle \boldsymbol{Q}_0'',\boldsymbol{q}_1'',\ldots,\boldsymbol{q}_N'' \middle| \hat{U}^\dagger\hat{U}F(\hat{\boldsymbol{Q}}_0,\hat{\boldsymbol{q}}_1,\ldots,\hat{\boldsymbol{q}}_N)\hat{U}^\dagger\hat{U} \middle| \boldsymbol{Q}_0',\boldsymbol{q}_1',\ldots,\boldsymbol{q}_N' \right\rangle \tag{2.176}$$

$$=\left(\left\langle \boldsymbol{Q}_0'',\boldsymbol{q}_1'',\ldots,\boldsymbol{q}_N'' \middle| \hat{U}^\dagger \right)F(A\hat{\boldsymbol{Q}}_0,A\hat{\boldsymbol{q}}_1,\ldots,A\hat{\boldsymbol{q}}_N)\left(\hat{U} \middle| \boldsymbol{Q}_0',\boldsymbol{q}_1',\ldots,\boldsymbol{q}_N' \right\rangle\right) \tag{2.177}$$

$$=|\mathcal{J}|^2 \langle \tilde{\boldsymbol{Q}}_0'',\tilde{\boldsymbol{q}}_1'',\ldots,\tilde{\boldsymbol{q}}_N''|F(A\hat{\boldsymbol{Q}}_0,A\hat{\boldsymbol{q}}_1,\ldots,A\hat{\boldsymbol{q}}_N)|\tilde{\boldsymbol{Q}}_0',\tilde{\boldsymbol{q}}_1',\ldots,\tilde{\boldsymbol{q}}_N'\rangle \tag{2.178}$$

$$=|\mathcal{J}|^2 \bar{F}(A\tilde{\boldsymbol{Q}}_0',A\tilde{\boldsymbol{q}}_1',\ldots,A\tilde{\boldsymbol{q}}_N')\langle \tilde{\boldsymbol{Q}}_0'',\tilde{\boldsymbol{q}}_1'',\ldots,\tilde{\boldsymbol{q}}_N''|\tilde{\boldsymbol{Q}}_0',\tilde{\boldsymbol{q}}_1',\ldots,\tilde{\boldsymbol{q}}_N'\rangle. \tag{2.179}$$

Noting that $F(\hat{\boldsymbol{Q}}_0,\hat{\boldsymbol{q}}_1,\ldots,\hat{\boldsymbol{q}}_N)$ is arbitrary and comparing Eqs. (2.171) and (2.179), we have

$$\bar{F}(\boldsymbol{Q}_0',\boldsymbol{q}_1',\ldots,\boldsymbol{q}_N') = \bar{F}(A\tilde{\boldsymbol{Q}}_0',A\tilde{\boldsymbol{q}}_1',\ldots,A\tilde{\boldsymbol{q}}_N'), \tag{2.180}$$

$$\langle \boldsymbol{Q}_0'',\boldsymbol{q}_1'',\ldots,\boldsymbol{q}_N''|\boldsymbol{Q}_0',\boldsymbol{q}_1',\ldots,\boldsymbol{q}_N'\rangle = |\mathcal{J}|^2 \langle \tilde{\boldsymbol{Q}}_0'',\tilde{\boldsymbol{q}}_1'',\ldots,\tilde{\boldsymbol{q}}_N''|\tilde{\boldsymbol{Q}}_0',\tilde{\boldsymbol{q}}_1',\ldots,\tilde{\boldsymbol{q}}_N'\rangle. \tag{2.181}$$

Equation ([2.180](#)) specifically means that

$$
\begin{bmatrix} \tilde{\boldsymbol{Q}}_0 \\ \tilde{\boldsymbol{q}}_1 \\ \vdots \\ \tilde{\boldsymbol{q}}_N \end{bmatrix} = A^{-1} \begin{bmatrix} \boldsymbol{Q}_0 \\ \boldsymbol{q}_1 \\ \vdots \\ \boldsymbol{q}_N \end{bmatrix} \tag{2.182}
$$

and therefore

$$
\langle \boldsymbol{Q}_0'', \boldsymbol{x}_1'', \ldots, \boldsymbol{x}_N'' | \boldsymbol{Q}_0', \boldsymbol{x}_1', \ldots, \boldsymbol{x}_N' \rangle \tag{2.183}
$$

$$
= |\mathcal{J}|^2 \langle A^{-1} \boldsymbol{Q}_0'', A^{-1} \boldsymbol{x}_1'', \ldots, A^{-1} \boldsymbol{x}_N'' | A^{-1} \boldsymbol{Q}_0', A^{-1} \boldsymbol{x}_1', \ldots, A^{-1} \boldsymbol{x}_N' \rangle \tag{2.184}
$$

$$
= \underbrace{|\mathcal{J}|^2 \det[A]}_{=1} \langle \boldsymbol{Q}_0'', \boldsymbol{x}_1'', \ldots, \boldsymbol{x}_N'' | \boldsymbol{Q}_0', \boldsymbol{x}_1', \ldots, \boldsymbol{x}_N' \rangle. \tag{2.185}
$$

Here, we used the general formula

$$
\langle A^{-1} \boldsymbol{Q}_0'', A^{-1} \boldsymbol{x}_1'', \ldots, A^{-1} \boldsymbol{x}_N'' | A^{-1} \boldsymbol{Q}_0', A^{-1} \boldsymbol{x}_1', \ldots, A^{-1} \boldsymbol{x}_N' \rangle \tag{2.186}
$$

$$
= \det[A] \langle \boldsymbol{Q}_0'', \boldsymbol{x}_1'', \ldots, \boldsymbol{x}_N'' | \boldsymbol{Q}_0', \boldsymbol{x}_1', \ldots, \boldsymbol{x}_N' \rangle. \tag{2.187}
$$

We then have

$$
|\mathcal{J}| = \frac{1}{\sqrt{\det[A]}} \tag{2.188}
$$

and obtain

$$
\hat{U} |\boldsymbol{Q}_0, \boldsymbol{x}_1, \ldots, \boldsymbol{x}_N \rangle = \frac{1}{\sqrt{\det[A]}} |A^{-1} \boldsymbol{Q}_0', A^{-1} \boldsymbol{x}_1', \ldots, A^{-1} \boldsymbol{x}_N' \rangle. \tag{2.189}
$$

Unitary representation of linear canonical transformation

Equations ([2.22](#)), ([2.23](#)), ([2.24](#)), and ([2.25](#)) give a type of linear canonical transformation represented by

$$
\begin{cases} \hat{\boldsymbol{q}} \mapsto \hat{\boldsymbol{Q}} := A\hat{\boldsymbol{q}} = \left(\sum_{j=1}^{f} A_{1,j} \hat{q}_j, \sum_{j=1}^{f} A_{2,j} \hat{q}_j, \ldots, \sum_{j=1}^{f} A_{f,j} \hat{q}_j \right), & \tag{2.190a} \\[3mm] \hat{\boldsymbol{p}} \mapsto \hat{\boldsymbol{P}} := B\hat{\boldsymbol{p}} = \left(\sum_{j=1}^{f} B_{1,j} \hat{p}_j, \sum_{j=1}^{f} B_{2,j} \hat{p}_j, \ldots, \sum_{j=1}^{f} B_{f,j} \hat{p}_j \right). & \tag{2.190b} \end{cases}
$$

46

Here $\hat{\boldsymbol{q}} = (\hat{q}_1, \hat{q}_2, \ldots, \hat{q}_f)^T$ and $\hat{\boldsymbol{p}} = (\hat{p}_1, \hat{p}_2, \ldots, \hat{p}_f)^T$ denote f-dimensional dynamical variables, each component of which satisfies

$$[\hat{q}_i, \hat{p}_j] = i\hbar \delta_{i,j}, \tag{2.191}$$

and A, B are real matrices. In this case, it holds that

$$AB^T = I, \tag{2.192}$$

where I is the identity matrix. We use the fact to prove that any linear canonical transformation accompanies the corresponding unitary representation.

To this end, we first show Eq. (2.192). Evaluating the commutation relation of the dynamical variables $(\hat{\boldsymbol{Q}}, \hat{\boldsymbol{P}})$, we have

$$\left[\hat{Q}_i, \hat{P}_j\right] = \left[\sum_{k=1}^{f} A_{i,k} \hat{q}_k, \sum_{l=1}^{f} B_{j,l} \hat{p}_l\right] \tag{2.193}$$

$$= \sum_{k=1}^{f} \sum_{l=1}^{f} A_{i,k} B_{j,l} \underbrace{\left[\hat{q}_k, \hat{p}_l\right]}_{=i\hbar\delta_{k,l}} \tag{2.194}$$

$$= i\hbar \sum_{k=1}^{f} A_{i,k} (B^T)_{k,j}. \tag{2.195}$$

If Eq. (2.190) gives a canonical transformation, it must also hold that

$$\left[\hat{Q}_i, \hat{P}_j\right] = i\hbar \delta_{i,j}. \tag{2.196}$$

We then have the condition

$$AB^T = I \tag{2.192}$$

for the matrices A, B to give a canonical transformation in the representation (2.190).

47

Using Eq. (2.192), we try to represent the transformation (2.190) by a unitary representation

$$
\begin{cases}
\hat{\boldsymbol{q}} \mapsto \hat{U}\hat{\boldsymbol{q}}\hat{U}^\dagger, & \text{(2.197a)} \\
\hat{\boldsymbol{p}} \mapsto \hat{U}\hat{\boldsymbol{p}}\hat{U}^\dagger & \text{(2.197b)}
\end{cases}
$$

with the ansatz

$$
\hat{U} = \exp\left[\frac{1}{2}\sum_{i=1}^{f}\sum_{j=1}^{f} c_{i,j}\left(\hat{q}_i\hat{p}_j + \hat{p}_j\hat{q}_i\right)/i\hbar\right] \equiv e^{\hat{\mathcal{G}}[\mathbf{c}]}. \tag{2.198}
$$

Here we demand that the generating matrix $c_{i,j}$ is real for the operator $\hat{U}$ to be unitary. First, the unitary operator (2.198) acts on $\hat{q}_i$ as follows:

$$
\hat{U}\hat{q}_i\hat{U}^\dagger = \sum_{k=0}^{\infty}\frac{1}{k!}\mathrm{ad}_{\hat{\mathcal{G}}[\mathbf{c}]}^{k}(\hat{q}_i). \tag{2.199}
$$

Here, we used the notation (2.109) and used the formula (2.108). We can evaluate the values of the array $\left\{\mathrm{ad}_{\hat{\mathcal{G}}[\mathbf{c}]}^{k}(\hat{q}_i)\right\}_{k=0}^{\infty}$ inductively as follows. For the case of $k = 0$, it holds that

$$
\mathrm{ad}_{\hat{\mathcal{G}}[\mathbf{c}]}^{0}(\hat{q}_i) = \hat{q}_i. \tag{2.200}
$$

For the case of $k = 1$, it holds that

$$
\mathrm{ad}_{\hat{\mathcal{G}}[\mathbf{c}]}^{1}(\hat{q}_i) = \left[\hat{\mathcal{G}}[\mathbf{c}], \mathrm{ad}_{\hat{\mathcal{G}}[\mathbf{c}]}^{0}(\hat{q}_i)\right] \tag{2.201}
$$

$$
= \frac{1}{2i\hbar}\sum_{j=1}^{f}\sum_{k=1}^{f} c_{j,k}\underbrace{\left[\hat{q}_j\hat{p}_k + \hat{p}_k\hat{q}_j, \hat{q}_i\right]}_{-2i\hbar\delta_{k,i}\hat{q}_j} \tag{2.202}
$$

$$
= \sum_{j=1}^{f}(-\mathbf{c})_{j,i}\hat{q}_j \tag{2.203}
$$

$$
= \sum_{j=1}^{f}(-\mathbf{c}^T)_{i,j}\hat{q}_j. \tag{2.204}
$$

Under the assumption that

$$\mathrm{ad}_{\hat{\mathcal{G}}[c]}^{k}(\hat{q}_i) = \sum_{j=1}^{f}\left[(-c^T)^k\right]_{i,j}\hat{q}_j \tag{2.205}$$

for a value of $k \geq 2$, it immediately follows that

$$\mathrm{ad}_{\hat{\mathcal{G}}[c]}^{k+1}(\hat{q}_i) = \left[\hat{\mathcal{G}}[c], \mathrm{ad}_{\hat{\mathcal{G}}[c]}^{k}(\hat{q}_i)\right] \tag{2.206}$$

$$= \frac{1}{2i\hbar}\sum_{k=1}^{f}\sum_{l=1}^{f}c_{k,l}\sum_{j=1}^{f}\left[(-c^T)^k\right]_{i,j}\underbrace{\left[\hat{q}_k\hat{p}_l + \hat{p}_l\hat{q}_k, \hat{q}_j\right]}_{-2i\hbar\delta_{k,i}\hat{q}_j} \tag{2.207}$$

$$= \sum_{k=1}^{f}(-c_{k,j})\sum_{j=1}^{f}\left[(-c^T)^k\right]_{i,j}\hat{q}_k \tag{2.208}$$

$$= \sum_{j=1}^{f}\sum_{k=1}^{f}\left[(-c^T)^k\right]_{i,j}\left[-c^T\right]_{j,k}\hat{q}_k \tag{2.209}$$

$$= \sum_{j=1}^{f}\left[(-c^T)^{k+1}\right]_{i,j}\hat{q}_j, \tag{2.210}$$

which fact is independent of the value of k. From the above, we have

$$\mathrm{ad}_{\hat{\mathcal{G}}[c]}^{k}(\hat{q}_i) = \sum_{j=1}^{f}\left[(-c^T)^k\right]_{i,j}\hat{q}_j \tag{2.211}$$

for all $k \geq 0$ and obtain

$$\left[\text{l.h.s of Eq. (2.199)}\right] = \sum_{k=0}^{\infty}\frac{1}{k!}\left\{\sum_{j=1}^{f}\left[(-c^T)^k\right]_{i,j}\hat{q}_j\right\} \tag{2.212}$$

$$= \sum_{j=1}^{f}\left[\exp\left(-c^T\right)\right]_{i,j}\hat{q}_j. \tag{2.213}$$

We can also evaluate the value of $\hat{U}\hat{p}_i\hat{U}^\dagger$ in the same way:

$$\hat{U}\hat{p}_i\hat{U}^\dagger = \sum_{k=0}^{\infty}\frac{1}{k!}\mathrm{ad}_{\hat{\mathcal{G}}[c]}^{k}(\hat{p}_i). \tag{2.214}$$

49

For the case of $k = 0$, we have

$$\text{ad}^0_{\hat{\mathcal{G}}[\mathsf{c}]}(\hat{p}_i) = \hat{p}_i. \tag{2.215}$$

For the case of $k = 1$, we have

$$\text{ad}^1_{\hat{\mathcal{G}}[\mathsf{c}]}(\hat{p}_i) = \left[\hat{\mathcal{G}}[\mathsf{c}], \text{ad}^0_{\hat{\mathcal{G}}[\mathsf{c}]}(\hat{p}_i)\right] \tag{2.216}$$

$$= \frac{1}{2i\hbar} \sum_{j=1}^{f} \sum_{k=1}^{f} c_{j,k} \underbrace{\left[\hat{q}_j\hat{p}_k + \hat{p}_k\hat{q}_j, \hat{p}_i\right]}_{2i\hbar\delta_{j,i}\hat{p}_k} \tag{2.217}$$

$$= \sum_{k=1}^{f} [\mathsf{c}]_{i,k}\hat{p}_k. \tag{2.218}$$

Here, assuming that

$$\text{ad}^k_{\hat{\mathcal{G}}[\mathsf{c}]}(\hat{p}_i) = \sum_{j=1}^{f} \left[\mathsf{c}^k\right]_{i,j}\hat{p}_j \tag{2.219}$$

for a value of $k \geq 2$, we immediately have

$$\text{ad}^{k+1}_{\hat{\mathcal{G}}[\mathsf{c}]}(\hat{p}_i) = \left[\hat{\mathcal{G}}[\mathsf{c}], \text{ad}^k_{\hat{\mathcal{G}}[\mathsf{c}]}(\hat{p}_i)\right] \tag{2.220}$$

$$= \frac{1}{2i\hbar} \sum_{k=1}^{f} \sum_{l=1}^{f} c_{k,l} \sum_{j=1}^{f} \left[\mathsf{c}^k\right]_{i,j} \underbrace{\left[\hat{q}_k\hat{p}_l + \hat{p}_l\hat{q}_k, \hat{p}_j\right]}_{-2i\hbar\delta_{k,j}\hat{p}_l} \tag{2.221}$$

$$= \sum_{j=1}^{f} c_{j,l} \sum_{l=1}^{f} \left[\mathsf{c}^k\right]_{i,j}\hat{p}_l \tag{2.222}$$

$$= \sum_{l=1}^{f} \sum_{j=1}^{f} \underbrace{\left[\mathsf{c}^k\right]_{i,j}[\mathsf{c}]_{j,l}}_{[\mathsf{c}^{k+1}]_{i,l}} \hat{p}_l \tag{2.223}$$

$$= \sum_{j=1}^{f} \left[\mathsf{c}^{k+1}\right]_{i,j}\hat{p}_j, \tag{2.224}$$

50

which fact is independent of the value of k. From the above, we have

$$\text{ad}^k_{\hat{\mathcal{G}}[\text{c}]}(\hat{p}_i) = \sum_{j=1}^{f} \left[\text{c}^k \right]_{i,j} \hat{p}_j \tag{2.225}$$

for all $k \geq 0$ and obtain

$$\left[\text{l.h.s of Eq. (2.214)} \right] = \sum_{k=0}^{\infty} \frac{1}{k!} \left\{ \sum_{j=1}^{f} \left[(-\text{c}^T)^k \right]_{i,j} \hat{p}_j \right\} \tag{2.226}$$

$$= \sum_{j=1}^{f} \left[\exp(\text{c}) \right]_{i,j} \hat{p}_j. \tag{2.227}$$

We then arrive at the condition

$$\begin{cases} \exp(\text{c}) = A, & \text{(2.228a)} \\ \exp\left(-\text{c}^T\right) = B. & \text{(2.228b)} \end{cases}$$

Note that the condition (2.228) is consistent with $AB^T = I$ because

$$\left[\exp(\text{c}) \right]^{-T} = \exp\left(-\text{c}^T\right). \tag{2.229}$$

Equation (2.198) and the additional condition (2.228) give the unitary representation of the linear canonical transformation (2.190).

Chapter 3

XXZ model with periodically driven exchange interactions

3.1 Background and motivation

Periodically driven quantum many-body systems constitute a class between time-independent systems and general time-dependent systems, having a mathematical structure that can be solved by reducing them to time-independent systems. This provides a hint for designing Hamiltonians with new quantum states as stationary states, which would not be realized in bare time-independent systems. This technique is called *Floquet engineering* in reference to the Floquet theory [69], which is a general theory for time-periodic systems and has contributed to generation of new gauge fields in the optical lattice [70–77] and deformation of the band structure of graphene [78–85], for example.

This study is a joint work with Seiji Yunoki (RIKEN, CEMS, as of December 2020) to be submitted (in preparation).

The starting point of the Floquet engineering is to represent the periodically driven system in terms of a time-independent effective Hamiltonian. Using the Floquet theory, given a time-periodic Hamiltonian $\hat{\mathcal{H}}(t) = \hat{\mathcal{H}}(t + T)$, we can construct a generator of time evolution over one cycle of $\hat{\mathcal{H}}(t)$, which is called the *Floquet Hamiltonian*. In the short-period limit $T \to 0$, or equivalently in the high-frequency limit $\Omega := 2\pi/T \to \infty$, the Floquet Hamiltonian coincides with the average Hamiltonian given by

$$\hat{\mathcal{H}}_{\mathrm{ave}} := \frac{1}{T} \int_0^T dt \, \hat{\mathcal{H}}(t). \tag{3.1}$$

Therefore, the average Hamiltonian is often referred to as the effective (Floquet) Hamiltonian and is denoted by $\hat{\mathcal{H}}_{\mathrm{eff}}$.

It is important, however, to note that we can in general obtain a number of effective Hamiltonians. In other words, for a given periodic Hamiltonian $\hat{\mathcal{H}}(t)$, there are a generally infinite number of effective Hamiltonians

$$\hat{\mathcal{H}}_{\mathrm{eff}} = \frac{1}{T} \int_0^T dt \, \hat{\mathcal{U}}(t)[\hat{\mathcal{H}}(t) - i\hbar \partial_t]\hat{\mathcal{U}}^\dagger(t), \tag{3.2}$$

each of which is specified by the unitary transformation $\hat{\mathcal{U}}(t)$. The average Hamiltonian (3.1) is only a spacial case in which $\hat{\mathcal{U}}(t)$ is the identity operator. Out of the infinitely large set $\{\hat{\mathcal{U}}(t)\}$, we should choose one that is appropriate to the purpose of research, especially when investigating nonlinear effects of driving forces in interacting many-body systems.

One example of such nonlinear effects is correlated tunneling in interacting bosons, which was predicted theoretically by Rapp *et al.* [86] for the Bose-Hubbard model with time-dependent on-site interactions and was demonstrated experimentally by Meinert *et al.* [87] using the corresponding cold-atom system. Correlated tunneling can only be described by $\hat{\mathcal{H}}_{\mathrm{eff}}$ under a specific choice of $\hat{\mathcal{U}}(t)$. The driven Bose-Hubbard model used in Refs. [86, 87] is given by the

time-dependent Hamiltonian

$$\hat{\mathcal{H}}(t) = -J \sum_{\langle i,j \rangle} \hat{a}_i^\dagger \hat{a}_j + \sum_i \frac{U(t)}{2} \hat{n}_i(\hat{n}_i - 1), \qquad (3.3)$$

where $\hat{a}_i^\dagger$ and $\hat{a}_i$ are the bosonic creation and annihilation operators at the site i, $\hat{n}_i = \hat{a}_i^\dagger \hat{a}_i$ is the number operator, and the on-site interaction $U(t)$ oscillates in time as $U(t) = \bar{U} + \delta U \sin \Omega t$. Adopting the unitary transformation

$$\hat{\mathcal{U}}(t) = \exp\left[\frac{1}{2i} \frac{\delta U}{\hbar \Omega} \cos \Omega t \sum_i \hat{n}_i(\hat{n}_i - 1) \right], \qquad (3.4)$$

we obtain the effective Hamiltonian

$$\hat{\mathcal{H}}_{\text{eff}} = -J \sum_{\langle i,j \rangle} \hat{a}_i^\dagger \mathcal{J}_0(\hat{A}_{i,j}) \hat{a}_j + \sum_i \frac{\bar{U}}{2} \hat{n}_i(\hat{n}_i - 1), \qquad (3.5)$$

where $\mathcal{J}_0(x)$ is the zeroth-order Bessel function of the first kind and

$$\hat{A}_{i,j} := (\delta U/\hbar \Omega) \times (\hat{n}_i - \hat{n}_j) \qquad (3.6)$$

is the scaled particle-number difference between sites i and j.

In this Hamiltonian, the elementary processes describing the movement of particles are governed by effective bond operator

$$\hat{b}_{i,j}^{(\text{eff})} := \hat{a}_i^\dagger \mathcal{J}_0(\hat{A}_{i,j}) \hat{a}_j + \text{h.c} \qquad (3.7)$$

for each bond (i, j). Let $n_i := \langle \Psi | \hat{n}_i | \Psi \rangle$ be the expectation value of the number operator $\hat{n}_i$ on site i under the state $|\Psi\rangle$. We can expect the dynamics through $\hat{A}_{i,j}$ due to the bond operator $\hat{b}_{i,j}^{(\text{eff})}$ depending on the spatial distribution of n_i. For example, for a bond (i, j), the process of changing the particle number distribution from $(n_i, n_j) = (0, 1)$ to $(n_i, n_j) = (1, 0)$ always takes place with a constant amplitude $-J$ because $\mathcal{J}_0(0) = 1$. On the other hand, for the same bond, the process of changing from $(n_i, n_j) = (1, 1)$ to $(n_i, n_j) = (2, 0)$ takes place with an amplitude $J \times \mathcal{J}_0(\delta U/\hbar \Omega)$. When the value of $(\delta U/\hbar \Omega)$ is set to a zero

of the Bessel function $\mathcal{J}_0(x)$, the latter process is strongly suppressed while the former process is intact. This complex state dependence is one of the features of correlated tunneling. If we averaged the original Hamiltonian $\hat{\mathcal{H}}(t)$ as in Eq. (3.1) by choosing the identity for $\hat{\mathcal{U}}(t)$, we would only find a trivial time-independent part of $\hat{\mathcal{H}}(t)$:

$$\hat{\mathcal{H}}_{\text{ave}} = -J \sum_{\langle i,j \rangle} \hat{a}_i^\dagger \hat{a}_j + \sum_i \frac{\bar{U}}{2} \hat{n}_i(\hat{n}_i - 1), \tag{3.8}$$

from which we would not be able to derive correlated tunneling. This demonstrates that the choice of $\hat{\mathcal{U}}(t)$ is essential for the observation of target phenomena.

When the total Hamiltonian is written as $\hat{\mathcal{H}}(t) = \hat{\mathcal{H}}_0 + \hat{\mathcal{V}}(t)$ such that $\int_0^{2\pi/\Omega} dt\, \hat{\mathcal{V}}(t) = 0$, we should utilize the unitary transformation in the form

$$\hat{\mathcal{U}}(t) = \mathcal{T} \exp\left[-\int^t \frac{dt'}{i\hbar} \hat{\mathcal{V}}(t') \right], \tag{3.9}$$

which reduces to Eq. (3.4) in the case of the Hamiltonian (3.3). Combining this with Eq. (3.2), we obtain the interaction term as in

$$\hat{\mathcal{V}}_{\text{eff}} := \frac{1}{T} \int_0^T dt\, [\hat{\mathcal{U}}(t) \hat{\mathcal{H}}_0 \hat{\mathcal{U}}^\dagger(t) - \hat{\mathcal{H}}_0]. \tag{3.10}$$

Note that the driving term in Eq. (3.3) acts on each site i, whereas the resulting interaction in Eq. (3.5) acts on each bond (i, j). This motivates us to investigate a possibility of finding, out of a driving two-body interaction, an effective long-range interaction of the form (3.10).

In the present study, we indeed find a four-site interaction out of an XXZ model in which the longitudinal exchange interaction is periodically driven with constant amplitude. In the resulting model, we observe a *state-selective localization*, that is, a limited number of Ising-like product states become fixed points of the dynamics generated by the effective Hamiltonian. This means

55

that under the basis of the Ising-like product states, we observe dynamics that strongly depends on the initial state. Such an initial-state-dependent dynamics has also been reported as the quantum scar, which is one of the mechanisms preventing the thermal equilibration of quantum many-body systems [88, 89].

3.2   Methods and Results

3.2.1   Emergent long-range interactions (Result I)

We consider an XXZ model with periodically driven longuitudinal exchange interactions on an arbitrary lattice, whose Hamiltonian is given by

$$\hat{\mathcal{H}}(t) = -\frac{J_\perp}{2} \sum_{\langle i,j \rangle} (\hat{S}_i^+ \hat{S}_j^- + \hat{S}_i^- \hat{S}_j^+) - J_\parallel(t) \sum_{\langle i,j \rangle} \hat{S}_i^z \hat{S}_j^z, \tag{3.11}$$

where $J_\perp$ and $J_\parallel(t) \equiv \bar{J}_\parallel + \delta J \cos \Omega t$ are the transverse and longuitudinal components of the exchange interaction, respectively, and $\{\hat{S}_i^{z,\pm}\}$ are the spin operators satisfying $[\hat{S}_i^+, \hat{S}_j^-] = \delta_{i,j} \hat{S}_i^z$ and $[\hat{S}_i^z, \hat{S}_\pm^{(j)}] = \pm \delta_{i,j} \hat{S}_\pm^{(i)}$. Here, the symbol $\sum_{\langle i,j \rangle}$ indicates summation over all the bonds on the lattice.

In the present case, for the unitary transformation (3.9) we choose

$$\hat{\mathcal{U}}(t) = \exp\left[-iA \sin \Omega t \sum_{\langle i,j \rangle} \hat{S}_i^z \hat{S}_j^z\right], \tag{3.12}$$

where

$$A := \frac{\delta J}{\hbar \Omega} \tag{3.13}$$

is the dimensionless amplitude of the driving force and thus the effective Hamiltonian (3.2) takes the form

$$\hat{\mathcal{H}}_{\text{eff}}(A) = -\frac{J_\perp}{2} \sum_{\langle i,j \rangle} \left[\hat{S}_i^+ \mathcal{J}_0(A\hat{Z}_{i,j})\hat{S}_j^- + \text{h.c.}\right] - \bar{J}_\parallel \sum_{\langle i,j \rangle} \hat{S}_i^z \hat{S}_j^z; \tag{3.14}$$

see App. 3.A for the derivation. Here,

$$\hat{Z}_{i,j} = \sum_{\langle k,\underline{i} \rangle} \hat{S}_k^z - \sum_{\langle k,\underline{j} \rangle} \hat{S}_k^z \tag{3.15}$$

is the local staggered magnetization around the bond (i,j). Note that $\sum_{\langle k,i \rangle} \hat{\mathcal{O}}_k$ denotes summation of $\hat{\mathcal{O}}_k$ for all sites that are connected to i.

The operator $\hat{Z}_{i,j}$ produces a new type of long-range interaction. First, the operator $\hat{Z}_{i,j}$ involves many spins that depends on the underlying lattice structure. In fact, if the lattice is given on a square lattice of dimension d, $\hat{Z}_{i,j}$ is written as the sum of $\hat{S}_k^z$ over $4d$ pieces of sites, since the coordination number is given by $2d$ (see Fig. 3.2.1). Second, $\hat{Z}_{i,j}$ has the following property. Let the value of the parameter A be one of the innumerable zeros of the Bessel function $\mathcal{J}_0(x)$, i.e., A_λ with $\mathcal{J}_0(A_\lambda) = 0$. If the operator $\hat{Z}_{i,j}$ produces the eigenvalue ± 1 in the argument of $\mathcal{J}_0(A_\lambda \hat{Z}_{i,j})$ when $\hat{\mathcal{H}}_{\text{eff}}(A_\lambda)$ acts on a quantum state $|\Psi\rangle$, then it holds that

$$\hat{\mathcal{H}}_{\text{eff}}(A_\lambda)|\Psi\rangle = -\bar{J}_\parallel \sum_{\langle i,j \rangle} \hat{S}_i^z \hat{S}_j^z |\Psi\rangle. \tag{3.16}$$

Since $\hat{Z}_{i,j}$ is written in terms of $\hat{S}_k^z$, let us choose the set of Ising-like product states as the representation basis hereafter. We can then classify all basis states into two types depending on the eigenvalue of $\hat{Z}_{i,j}$, states for which the eigenvalue is either 1 or -1 and hence Eq. (3.16) holds, and the other states for which Eq. (3.16) does not hold.

We formulate it more specifically as follows. First, we break down the Hamiltonian into two terms:

$$\hat{\mathcal{H}}_{\text{eff}}(A) = \hat{\mathcal{H}}_{\text{eff}}^{XY}(A) + \hat{\mathcal{H}}^{\text{Ising}}, \tag{3.17}$$
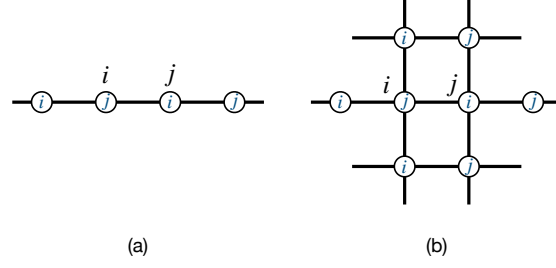
Figure 3.2.1: Range of action of $\hat{Z}_{i,j}$ for a bond (i,j) in (a) a one-dimensional chain and (b) a two-dimensional square lattice. The gray letters inside the circles indicate the sites they are connected to either site i or site j.

where

$$\hat{\mathcal{H}}_{\text{eff}}^{XY}(A) := -\frac{J_\perp}{2} \sum_{\langle i,j \rangle} \left[\hat{S}_i^+ \mathcal{J}_0(A\hat{Z}_{i,j})\hat{S}_j^- + (+ \leftrightarrow -) \right] \tag{3.18}$$

$$\hat{\mathcal{H}}^{\text{Ising}} := -\bar{J}_\parallel \sum_{\langle i,j \rangle} \hat{S}_i^z \hat{S}_j^z. \tag{3.19}$$

Let $\mathfrak{H}^{\text{Ising}}$ be the set of Ising-like product states that can be realized on a given lattice; see Eq. (3.25) below for an example of $S = 1/2$. Then an arbitrary state $|\Psi\rangle \in \mathfrak{H}^{\text{Ising}}$ can be classified into two types depending on whether or not it satisfies the vanishing condition

$$\hat{\mathcal{H}}_{\text{eff}}^{XY}(A_\lambda)|\Psi\rangle = 0. \tag{3.20}$$

Let $\mathfrak{H}_0^{\text{Ising}}$ be the set of the former, and $\mathfrak{H}_1^{\text{Ising}}$ be the set of the latter. The condition (3.20) gives the decomposition into the direct sum $\mathfrak{H}^{\text{Ising}} = \mathfrak{H}_0^{\text{Ising}} \oplus \mathfrak{H}_1^{\text{Ising}}$. By casting the condition (3.20) into the form

$$\exp\left[\frac{1}{i\hbar} \hat{\mathcal{H}}_{\text{eff}}(A_\lambda) \times t \right]|\Psi\rangle \propto |\Psi\rangle \tag{3.21}$$

for an arbitrary $t \in \mathbb{R}$, we realize that the state $|\Psi\rangle \in \mathfrak{H}_0^{\text{Ising}}$ is a fixed point of the dynamics generated by $\hat{\mathcal{H}}_{\text{eff}}(A_\lambda)$. In other words, $\hat{\mathcal{H}}_{\text{eff}}(A)$ creates dynamics such that only the states $|\Psi\rangle \in \mathfrak{H}_0^{\text{Ising}}$ are selectively localized.

58

3.2.2 Spin-1/2 chain: analytical discussion (Result II)

In order to investigate the state-selective localization more specifically, we now analyze an $S = 1/2$ chain of length L under the periodic boundary condition. The two terms (3.18) and (3.19) in the effective Hamiltonian (3.14) now reads

$$\hat{\mathcal{H}}_{\text{eff}}^{XY}(A) = -\frac{J_\perp}{2} \sum_{i=1}^{L} \left[\hat{S}_i^+ \mathcal{J}_0(A\hat{Z}_{i,i+1}) \hat{S}_{i+1}^- + (+ \leftrightarrow -) \right] \tag{3.22}$$

$$\hat{\mathcal{H}}^{\text{Ising}} = -\bar{J}_\parallel \sum_{i=1}^{L} \hat{S}_i^z \hat{S}_{i+1}^z, \tag{3.23}$$

respectively, where $\hat{S}_{L+1} = \hat{S}_1$ and

$$\hat{Z}_{i,i+1} = \hat{S}_{i-1}^z - \hat{S}_i^z + \hat{S}_{i+1}^z - \hat{S}_{i+2}^z. \tag{3.24}$$

Let us denote each element of $\mathfrak{H}^{\text{Ising}}$ as

$$|\Psi_{\boldsymbol{m}}\rangle = \bigotimes_{l=1}^{L} |m_i\rangle = |m_1, m_2, \dots, m_L\rangle, \tag{3.25}$$

where $|m_j\rangle$ is either of the local eigenstates $|+\rangle, |-\rangle$ defined by $\hat{S}_j^z |\pm\rangle = \pm |\pm\rangle/2$ and $\boldsymbol{m} = (m_1, m_2, \dots, m_L)$ in the label of the state $|\Psi_{\boldsymbol{m}}\rangle$. In this case, the condition (3.20) for $|\Psi\rangle$ is equivalent to the condition

$$\hat{b}_{i,i+1}(A_\lambda) |\Psi_{\boldsymbol{m}}\rangle = 0 \tag{3.26}$$

for every bond $(i, i+1)$, where we introduced the effective bond operator

$$\hat{b}_{i,i+1}(A) := \hat{S}_i^+ \mathcal{J}_0(A\hat{Z}_{i,i+1}) \hat{S}_{i+1}^- + (+ \leftrightarrow -) \tag{3.27}$$

Since the bond operator $\hat{b}_{i,i+1}$ acts on the four spins at $i-1, i, i+1, i+2$, we can focus on the 16 pieces of four-site states

$$|\psi_{i,i+1}\rangle = |m_{i-1}, m_i, m_{i+1}, m_{i+2}\rangle, \tag{3.28}$$

59

out of the state $|\Psi_{\boldsymbol{m}}\rangle$ given by

$$|\Psi_{\boldsymbol{m}}\rangle = |m_1, \ldots, m_{i-2}\rangle \otimes |\psi_{i,i+1}\rangle \otimes |m_{i+3}, \ldots, m_L\rangle, \tag{3.29}$$

reducing the condition (3.26) to

$$\hat{b}_{i,i+1}(A_\lambda)|\psi_{i,i+1}\rangle = 0. \tag{3.30}$$

First, we can classify the 16 four-site states into two groups: a group of 8 states satisfying $|m_{i+1}\rangle = |+\rangle$ and a group of 8 states satisfying $|m_{i+1}\rangle = |-\rangle$. For any state $|\psi_{i,i+1}\rangle$ in the former group, it holds that

$$\hat{b}_{i,i+1}(A)|\psi_{i,i+1}\rangle = \hat{S}_i^+ \mathcal{J}_0(A\hat{Z}_{i,i+1})\hat{S}_{i+1}^- |\psi_{i,i+1}\rangle. \tag{3.31}$$

In this case, since $\hat{S}_{i+1}^- |\psi_{i,i+1}\rangle$ is also one of the 16 four-site states, it is an eigenstate of $\mathcal{J}_0(A\hat{Z}_{i,i+1})$, and thus we have

$$\hat{S}_i^+ \mathcal{J}_0(A\hat{Z}_{i,i+1})\hat{S}_{i+1}^- |\psi_{i,i+1}\rangle \propto \hat{S}_i^+ \hat{S}_{i+1}^- |\psi_{i,i+1}\rangle \tag{3.32}$$

with the corresponding eigenvalue as the proportionality factor. In the same way, for any state $|\psi_{i,i+1}\rangle$ in the latter group, since it holds that

$$\hat{b}_{i,i+1}(A)|\psi_{i,i+1}\rangle = \hat{S}_i^- \mathcal{J}_0(A\hat{Z}_{i,i+1})\hat{S}_{i+1}^+ |\psi_{i,i+1}\rangle. \tag{3.33}$$

and since $\hat{S}_{i+1}^+ |\psi_{i,i+1}\rangle$ is an eigenstate of $\mathcal{J}_0(A\hat{Z}_{i,i+1})$, we have

$$\hat{S}_i^- \mathcal{J}_0(A\hat{Z}_{i,i+1})\hat{S}_{i+1}^+ |\psi_{i,i+1}\rangle \propto \hat{S}_i^- \hat{S}_{i+1}^+ |\psi_{i,i+1}\rangle. \tag{3.34}$$

Putting these two together, we obtain

$$\hat{b}_{i,i+1}(A)|\psi_{i,i+1}\rangle = \bar{\mathcal{J}} \times \hat{b}_{i,i+1}(0)|\psi_{i,i+1}\rangle \tag{3.35}$$

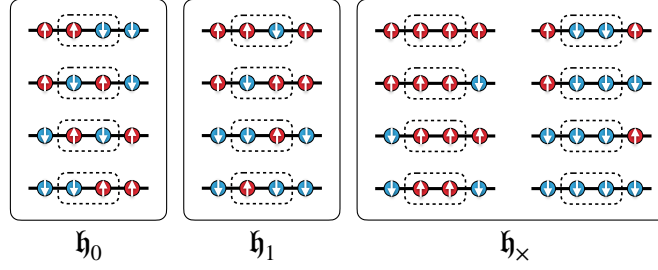with the proportionality coefficient $\bar{\mathcal{J}}$.

Figure 3.2.2: Classification of $2^4 = 16$ possible Ising-like product states in four consecutive sites (a cluster). The three groups $\mathfrak{h}_0$, $\mathfrak{h}_1$, and $\mathfrak{h}_\times$ shown in the figure correspond to the states given by Eqs. (3.36), (3.37), and (3.38), respectively. In each cluster state, the two sites enclosed in a dashed rectangle correspond to the bond $(i, i+1)$.

Table 3.2.1: The right-hand side of Eq. (3.35) for cases $\left|\psi_{i,i+1}\right\rangle \in \mathfrak{h}_0, \mathfrak{h}_1, \mathfrak{h}_\times$.

	$\bar{\mathcal{J}}$	$\hat{b}_{i,i+1}(0)\left|\psi_{i,i+1}\right\rangle$	$\bar{\mathcal{J}} \times \hat{b}_{i,i+1}(0)\left|\psi_{i,i+1}\right\rangle$
$\left|\psi_{i,i+1}\right\rangle \in \mathfrak{h}_0$	$\mathcal{J}_0(A)$	$\in \mathfrak{h}_0$	$\in \mathcal{J}_0(A)\mathfrak{h}_0$
$\left|\psi_{i,i+1}\right\rangle \in \mathfrak{h}_1$	1	$\in \mathfrak{h}_1$	$\in \mathfrak{h}_1$
$\left|\psi_{i,i+1}\right\rangle \in \mathfrak{h}_\times$	It depends.	0	0

We then classify the 16 four-site states further into three groups; see Fig. 3.2.2:

$$\mathfrak{h}_0 := \{|+,+,-,-\rangle, |+,-,+,-\rangle, |-,+,-,+\rangle, |-,-,+,+\rangle\}, \tag{3.36}$$

$$\mathfrak{h}_1 := \{|+,+,-,+\rangle, |+,-,+,+\rangle, |-,-,+,-\rangle, |-,+,-,-\rangle\}, \tag{3.37}$$

$$\mathfrak{h}_\times := \{|m_{i-1},+,+,m_{i+2}\rangle, |m_{i-1},-,-,m_{i+2}\rangle\}_{m_{i-1}=\pm, m_{i+2}=\pm}. \tag{3.38}$$

The behavior of $\bar{\mathcal{J}}$, $\hat{b}_{i,i+1}(0)\left|\psi_{i,i+1}\right\rangle$, and $\bar{\mathcal{J}} \times \hat{b}_{i,i+1}(0)\left|\psi_{i,i+1}\right\rangle$ on the right-hand side of Eq. (3.35) is shown in Table 3.2.1. Therefore, setting $A = A_\lambda$ yields

$$\hat{b}_{i,i+1}(A_\lambda)|\psi_{i,i+1}\rangle = \begin{cases} 0 & \text{for } |\psi_{i,i+1}\rangle \in \mathfrak{h}_0 \oplus \mathfrak{h}_\times \\ \hat{b}_{i,i+1}(0)|\psi_{i,i+1}\rangle & \text{for } |\psi_{i,i+1}\rangle \in \mathfrak{h}_1. \end{cases} \tag{3.39}$$

From the above, we know that the four-site state $|\psi_{i,i+1}\rangle$ satisfying the local vanishing condition (3.30) is given by the union set $\mathfrak{h}_0 \oplus \mathfrak{h}_\times$. On this basis, we can also construct a state $|\Psi_m\rangle$ that satisfies the global vanishing condition (3.20). In the next section, we verify numerically that such a state $|\Psi_m\rangle$ actually satisfies Eq. (3.20).

3.2.3 Spin-$1/2$ chain: numerical discussion (Result III)

Let us consider the following two product states:

$$|A_0\rangle = |-,-,-,-,-,-,-,-,+,+,+,+,+,+,+,+\rangle, \tag{3.40}$$

$$|A_1\rangle = |-,-,-,-,-,-,-,\underline{+,-},+,+,+,+,+,+,+\rangle \tag{3.41}$$

on $L = 16$ finite-size chain. The former (3.40) is a state with one domainwall at the bond $(8, 9)$ and is contained in $\mathfrak{H}_0^{\text{Ising}}$ because $|\psi_{n,n+1}\rangle \in \mathfrak{h}_\times \oplus \mathfrak{h}_0$ holds for every bond $(n, n+1) \in E$. The latter (3.41) is a state in which the spins at the bond $(8, 9)$ (the position that the underline indicates) are flipped and is contained in $\mathfrak{H}_1^{\text{Ising}}$ because the bonds $(7, 8)$ and $(9, 10)$ satisfy $|\psi_{7,8}\rangle \in \mathfrak{h}_1$ and $|\psi_{9,10}\rangle \in \mathfrak{h}_1$.

These two states $|A_0\rangle$ and $|A_1\rangle$ only differ in the partial state at the bond $(9, 10)$, which may be negligible in the thermodynamic limit $L \to \infty$. The slight difference, nevertheless, generates largely different time-evolution dynamics due to the fact that one state belongs to $\mathfrak{H}_0^{\text{Ising}}$ and the other state belongs to $\mathfrak{H}_1^{\text{Ising}}$. To see this, we estimate the value of $S_n^z(t) := \langle \Psi(t)| \hat{S}_n^z |\Psi(t)\rangle$ and the half-chain entanglement entropy given by

$$S_{L/2}(t) := \text{Tr}\left[-\hat{\rho}_{L/2}(t)\log\hat{\rho}_{L/2}(t)\right], \tag{3.42}$$

62

where

$$\hat{\rho}_{L/2}(t) := \text{Tr}_{1 \le n \le L/2}\Big[\big|\Psi(t)\big\rangle\big\langle\Psi(t)\big|\Big]. \tag{3.43}$$

The state vector at time t is given by

$$|\Psi(t)\rangle = \mathcal{T}\exp\left[\int_0^t \frac{dt'}{i\hbar}\hat{\mathcal{H}}(t')\right]|\Psi(0)\rangle, \tag{3.44}$$

which we numerically estimated by the package QuSpin [90, 91]. We chose the parameters in the Hamiltonian $\hat{\mathcal{H}}(t)$ so that the effective Hamiltonian $\hat{\mathcal{H}}_{\text{eff}}(A_\lambda)$ well approximates the dynamics and that the condition $\mathcal{J}_0(A_\lambda) \simeq 0$ holds.

Figure 3.2.3 shows our estimates of the spatial profile of $S_i^z(t)$ at several times for the initial states $|A_0\rangle$ and $|A_1\rangle$ and for the frequencies $\Omega = 10.0, 8.0, 6.0, 4.0$. The difference in them demonstrates that the change from $|A_0\rangle$ to $|A_1\rangle$ makes a significant difference in the time evolution; the spin configuration remains almost constant for $|A_0\rangle$ but decays for $|A_1\rangle$. This is a direct consequence of the fact that the initial state $|A_0\rangle$ is a fixed point of the dynamics.

Figure 3.2.4 shows the time evolution of $S_{L/2}(t)$ for the same set of initial states and the frequencies $\Omega = 10.0, 8.0, 6.0, 4.0$. Each of the panels (a) and (b) shows a plateau-like behavior, which is considered as a kind of Floquet prethermalization, and indicates the scope how precisely the effective Hamiltonian $\hat{\mathcal{H}}_{\text{eff}}(A_\lambda)$ captures the time evolution.

We made a similar estimation for the following two product states:

$$|B_0\rangle = |-,-,-,-,+,+,+,+,-,-,-,-,+,+,+,+\rangle, \tag{3.45}$$

$$|B_1\rangle = |-,-,-,-,+,+,+,\underline{-,+},-,-,-,+,+,+,+\rangle. \tag{3.46}$$

These also form a situation that one belongs to $\mathfrak{h}_0$ and the other belongs $\mathfrak{h}_1$ with a slight difference at the bond $(8,9)$ (the position where the underline in Eq. (3.46) indicates). Figure 3.2.5 shows estimates of the spatial profile of $S_i^z(t)$
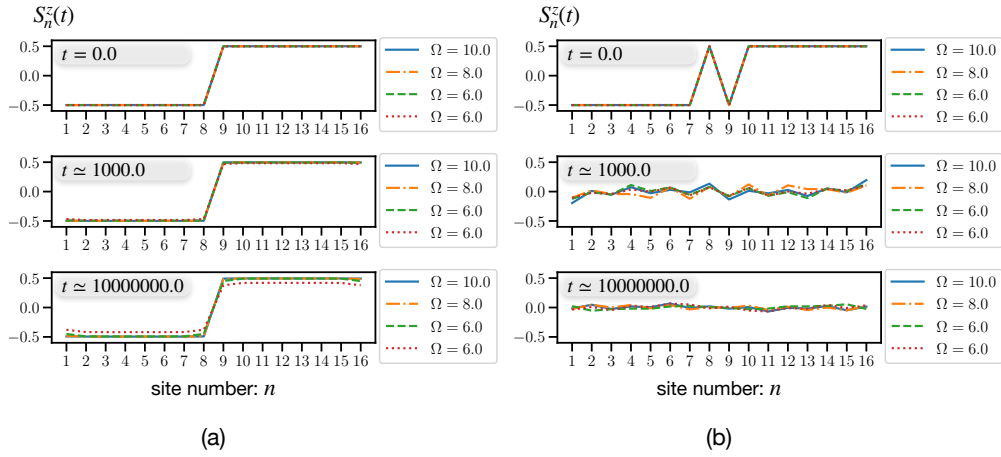
Figure 3.2.3: Numerical estimation of $S_i^z(t)$. Here, the value of $S_i^z(t) = +0.5$ corresponds to the spin state $|+\rangle$, while the value of $S_i^z(t) = -0.5$ corresponds to the spin state $|-\rangle$. The calculation conditions are set so that $A = 2.4048$, and hence $\mathcal{J}_0(A) \simeq 0$ holds with the fixed values $J_\parallel = -1.0$, $J_\perp = -0.75$ and $\hbar = 1$. The left panel (a) shows the result for the initial state $|\Psi(0)\rangle = |A_0\rangle$ and the right panel (b) shows that for the initial state $|\Psi(0)\rangle = |A_1\rangle$.
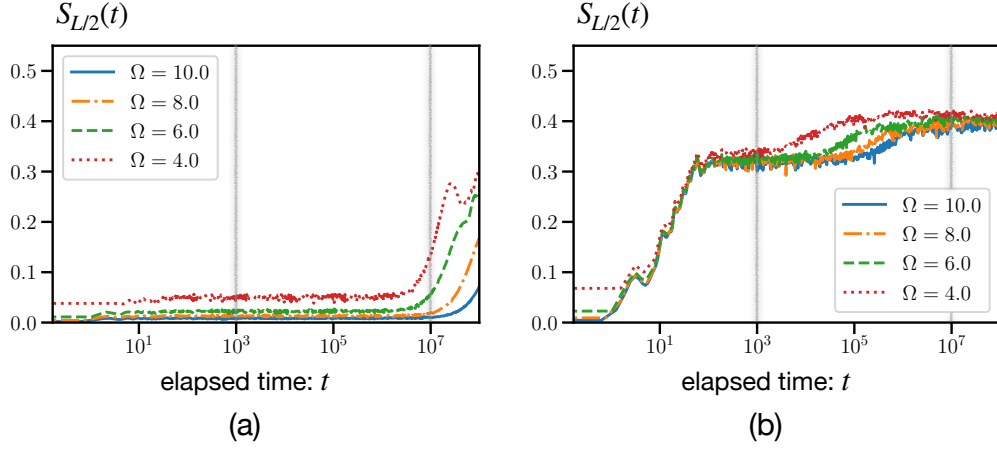
Figure 3.2.4: Numerical estimation of $S_{L/2}(t)$. The calculation conditions are the same as that of Fig. 3.2.3. The left panel (a) shows the result for the initial state $|\Psi(0)\rangle = |A_0\rangle$ and the right panel (b) shows that for the initial state $|\Psi(0)\rangle = |A_1\rangle$. The gray vertical lines indicate the times when we took the snapshots shown in Fig. 3.2.3.

at several times for the initial states $|B_0\rangle$ and $|B_1\rangle$ and for the frequencies $\Omega = 10.0, 8.0, 6.0, 4.0$. Figure 3.2.6 shows the time evolution of $S_{L/2}(t)$ for the same set of initial states and the frequencies $\Omega = 10.0, 8.0, 6.0, 4.0$. The behaviors shown in Figs. 3.2.5 and 3.2.6 are qualitatively similar to those in Figs. 3.2.3 and 3.2.4.

The results implies that by flipping a pair of spins on a bond we can switch the total state back and forth between $\mathfrak{H}_0^{\text{Ising}}$ and $\mathfrak{H}_1^{\text{Ising}}$. Hence, it is also possible to guess from the measurement of $S_i^z(t)$ whether the initial state $|\Psi(0)\rangle$ belongs to $\mathfrak{H}_0^{\text{Ising}}$ or $\mathfrak{H}_1^{\text{Ising}}$.
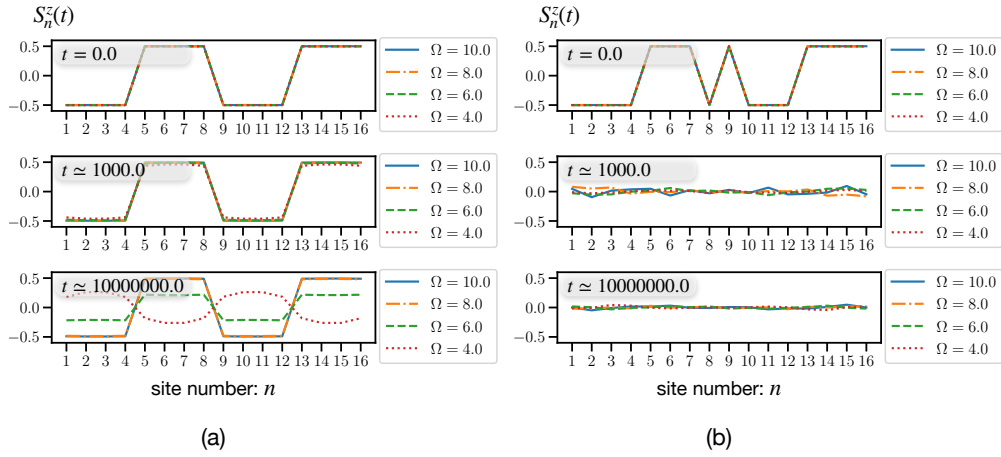
Figure 3.2.5: Numerical estimation of $S_i^z(t)$. Here, the value of $S_i^z(t) = +0.5$ corresponds to the spin state $|+\rangle$, while the value of $S_i^z(t) = -0.5$ corresponds to the spin state $|-\rangle$. The calculation conditions are set so that $A = 2.4048$, and hence $\mathcal{J}_0(A) \simeq 0$ holds with the fixed values $J_{\parallel} = -1.0$, $J_{\perp} = -0.75$ and $\hbar = 1$. The left panel (a) shows the result for the initial state $|\Psi(0)\rangle = |B_0\rangle$ and the right panel (b) shows that for the initial state $|\Psi(0)\rangle = |B_1\rangle$.
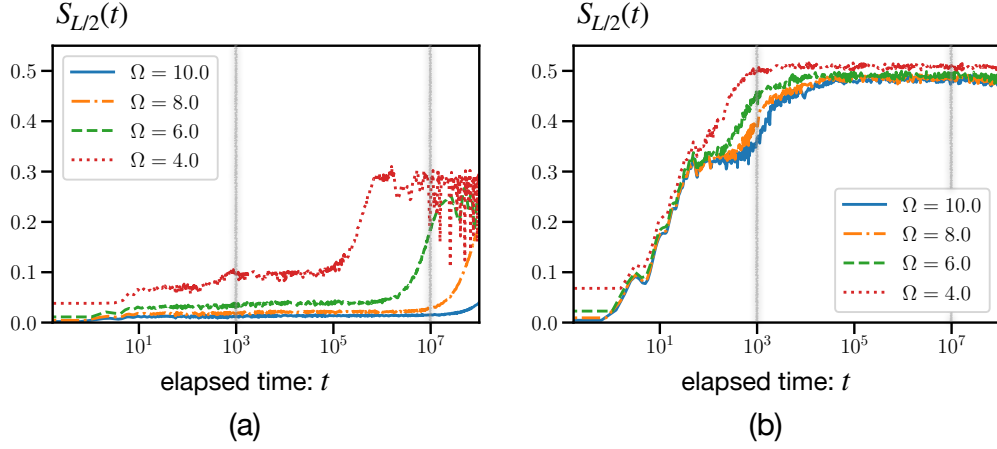
Figure 3.2.6: Numerical estimation of $S_{L/2}(t)$. The calculation conditions are same as that of Fig. 3.2.5. The left panel (a) shows the result for the initial state $|\Psi(0)\rangle = |B_0\rangle$ and the right panel (b) shows that for the initial state $|\Psi(0)\rangle = |B_1\rangle$. The gray vertical lines indicate the times when we took the snapshots shown in Fig. (3.2.5).

3.3   Summary

In the present work, we show that driven longitudinal exchange interactions in the *XXZ* model lead to long-range transverse exchange interactions in the Floquet picture, and results in a state-selective localization in which limited Ising-like product states are fixed points of the dynamics. Especially in the one-dimensional case with $S = 1/2$ and arbitrary length L, we show the long-range transverse interactions reduce to four-site interactions and specify the condition for a given Ising-like product state to be the fixed point. We also show some examples of such a localizable product state and numerically verified that these are actually fixed points of the dynamics.

   The driving protocol presented in the present study may be experimentally realized in magnetic insulators by a technique of controlling magnetism with ultrafast electric fields [92]. In addition to such experimental approaches, it is

also interesting to investigate the state-selective localization as a quantum scar [88, 89], which prevents thermal equilibration in isolated quantum many-body systems. The state-selective localization proposed in this study has a common feature to the quantum scar in that the dynamics is strongly dependent on the initial state. It is desirable that the model given in this study be properly extended to describe experimental situations and to investigate the quantum scar in more details.

Appendix

3.A Derivation of the Effective Hamiltonian

In this appendix, we present a detailed derivation for $\hat{\mathcal{H}}_{\text{eff}}(A)$ in Sec. 3.2.1. First, we decompose the original Hamiltonian given by Eq. (3.11) into $\hat{\mathcal{H}}(t) = \hat{\mathcal{H}}_0 + \hat{\mathcal{V}}(t)$ such that $\int_0^{2\pi/\Omega} dt\, \hat{\mathcal{V}}(t) = 0$ holds. Then, for

$$\hat{\mathcal{H}}_0 = -\frac{J_\perp}{2} \sum_{\langle i,j \rangle} (\hat{S}_i^+ \hat{S}_j^- + \hat{S}_i^- \hat{S}_j^+) - \bar{J}_\parallel \sum_{\langle i,j \rangle} \hat{S}_i^z \hat{S}_j^z, \tag{3.47}$$

$$\hat{\mathcal{V}}(t) = -\delta J \cos\Omega t \sum_{\langle i,j \rangle} \hat{S}_i^z \hat{S}_j^z, \tag{3.48}$$

we find the unitary transformation (3.9) in the form

$$\hat{\mathcal{U}}(t) = \mathcal{T} \exp\left[-\int^t \frac{dt'}{i\hbar} \hat{\mathcal{V}}(t')\right] \tag{3.49}$$

$$= \exp\left[-iA \sin\Omega t \sum_{\langle k,l \rangle} \hat{S}_k^z \hat{S}_l^z\right], \tag{3.50}$$

where A is given by Eq. (3.13). We then find Eq. (3.14) by substituting it into the formula

$$\hat{\mathcal{H}}_{\text{eff}}(A) = \frac{\Omega}{2\pi} \int_0^{2\pi/\Omega} dt\, \hat{\mathcal{U}}(t) \hat{\mathcal{H}}_0 \hat{\mathcal{U}}^\dagger(t). \tag{3.51}$$

Let us thereby evaluate $\hat{\mathcal{U}}(t) \hat{\mathcal{H}}_0 \hat{\mathcal{U}}^\dagger(t)$. Because of the commutation relation $[\hat{S}_i^z, \hat{\mathcal{U}}(t)] = 0$, we obtain

$$\hat{\mathcal{U}}(t) \hat{\mathcal{H}}_0 \hat{\mathcal{U}}^\dagger(t) = -\frac{J_\perp}{2} \sum_{\langle i,j \rangle} \hat{\mathcal{U}}(t) \left(\hat{S}_i^+ \hat{S}_j^- + \hat{S}_i^- \hat{S}_j^+\right) \hat{\mathcal{U}}^\dagger(t) - \bar{J}_\parallel \sum_{\langle i,j \rangle} \hat{S}_i^z \hat{S}_j^z. \tag{3.52}$$

69

Furthermore, using the formula

$$\mathrm{e}^{-i\hat{A}}\hat{B}\mathrm{e}^{i\hat{A}} = \sum_{n=0}^{\infty} \frac{(-i)^n}{n!}\left(\mathrm{ad}\hat{A}\right)^n \hat{B}, \tag{3.53}$$

where $\mathrm{ad}\hat{A} \cdot \hat{B} := [\hat{A}, \hat{B}]$, for any pair of operators $\hat{A}$ and $\hat{B}$, one of the terms in the square parentheses in Eq. (3.52) can be written as

$$\hat{\mathcal{U}}(t)\hat{S}_i^+\hat{S}_j^-\hat{\mathcal{U}}^\dagger(t) = \sum_{n=0}^{\infty} \frac{(-i)^n}{n!}(A\sin\Omega t)^n\left(\mathrm{ad}\sum_{\langle k,l\rangle}\hat{S}_z^{(k)}\hat{S}_l^z\right)^n\left(\hat{S}_i^+\hat{S}_j^-\right) \tag{3.54}$$

$$= \sum_{n=0}^{\infty} \frac{(-i)^n}{n!}(A\sin\Omega t)^n\hat{S}_i^+(\hat{Z}_{i,j})^n\hat{S}_j^- \tag{3.55}$$

$$= \hat{S}_i^+\exp\left[-iA\sin\Omega t \times \hat{Z}_{i,j}\right]\hat{S}_j^-, \tag{3.56}$$

where $\hat{Z}_{i,j}$ is given by Eq. (3.15).

We can prove the equality between Eqs. (3.54) and (3.55) by induction as follows. If we accept

$$\left(\mathrm{ad}\sum_{\langle k,l\rangle}\hat{S}_z^{(k)}\hat{S}_l^z\right)^m\left(\hat{S}_i^+\hat{S}_j^-\right) = \hat{S}_i^+(\hat{Z}_{i,j})^m\hat{S}_j^- \tag{3.57}$$

for a non-negative integer m, we obtain

$$\left(\mathrm{ad}\sum_{\langle k,l\rangle}\hat{S}_z^{(k)}\hat{S}_l^z\right)^{m+1}\left(\hat{S}_i^+\hat{S}_j^-\right) = \sum_{\langle k,l\rangle}[\hat{S}_z^{(k)}\hat{S}_l^z, \hat{S}_i^+(\hat{Z}_{i,j})^m\hat{S}_j^-] \tag{3.58}$$

$$= 2 \times \hat{S}_i^+\left[\sum_{\langle k,l\rangle}\left(\delta_{l,i} - \delta_{l,j}\right)\hat{S}_z^{(k)}\right](\hat{Z}_{i,j})^m\hat{S}_j^- \tag{3.59}$$

$$= \hat{S}_i^+(\hat{Z}_{i,j})^{m+1}\hat{S}_j^-. \tag{3.60}$$

For the equality between Eq. (3.58) and Eq. (3.59), we mainly use the symmetry of exchanging the indices k and l. For the equality between Eq. (3.59) and Eq. (3.60), we use the decomposition of the sum given by

$$2 \times \sum_{\langle k,l\rangle}\hat{\mathcal{O}}_{k,l} = \sum_k\sum_{\langle \underline{k},l\rangle}\hat{\mathcal{O}}_{k,l}, \tag{3.61}$$

70

where $\sum_{\langle k,i \rangle} \hat{\mathcal{O}}_k$ denotes summation of $\hat{\mathcal{O}}_k$ for all sites that are connected to i. Since Eq. (3.57) trivially holds for $m = 0$, it holds for any non-negative integers.

In exactly the same way, we obtain

$$\hat{\mathcal{U}}(t)\hat{S}_i^-\hat{S}_j^+\hat{\mathcal{U}}^\dagger(t) = \hat{S}_i^- \exp\left[+iA\sin\Omega t \times \hat{Z}_{i,j}\right]\hat{S}_j^+. \tag{3.62}$$

Hence, we find

$$\hat{\mathcal{U}}(t)\hat{\mathcal{H}}_0\hat{\mathcal{U}}^\dagger(t) = -\frac{J_\perp}{2} \sum_{\langle i,j \rangle}\left[\hat{S}_i^+ e^{-iA\sin\Omega t \times \hat{Z}_{i,j}}\hat{S}_j^- + (+ \leftrightarrow -)\right] - \bar{J}_\parallel \sum_{\langle i,j \rangle}\hat{S}_i^z\hat{S}_j^z. \tag{3.63}$$

Using the integral formula [93]

$$\frac{1}{2\pi}\int_0^{2\pi} d\theta\, e^{-ia\sin\theta} = \mathcal{J}_0(a), \quad \text{for } a \in \mathbb{R} \tag{3.64}$$

in Eq. (3.63), we arrive at

$$\hat{\mathcal{H}}_{\text{eff}}(A) = \frac{\Omega}{2\pi}\int_0^{2\pi/\Omega} dt\, \hat{\mathcal{U}}(t)\hat{\mathcal{H}}_0\hat{\mathcal{U}}^\dagger(t). \tag{3.65}$$

$$= -\frac{J_\perp}{2}\sum_{\langle i,j \rangle}\left[\hat{S}_i^+ \mathcal{J}_0(A\hat{Z}_{i,j})\hat{S}_j^- + (+ \leftrightarrow -)\right] - \bar{J}_\parallel\sum_{\langle i,j \rangle}\hat{S}_i^z\hat{S}_j^z, \tag{3.66}$$

where $\mathcal{J}_0(x)$ is the zeroth-order Bessel function of the first kind.

Chapter 4

Conclusion

4.1   Summary and Conclusion

In this thesis, we have shown that proper modeling of quantum-classical coupled systems allows us to theorize several experimental results and predict new phenomena. In Chapter 2, we derived an effective Hamiltonian for two-dimensional ^{4}He coupled with a movable platform and obtained an effective-mass formula from the platform's equation of motion. In Chapter 3, we showed that long-range interactions that emerge in a spin system lead to initial-state-sensitive dynamics.

In quantum-classical coupled systems, as introduced in Chapter 1, it is often crucial to derive the coupling Hamiltonian correctly. For such problems, Chapter 2 provides a straight-forward solution. We derived the Hamiltonian for two-dimensional ^{4}He fixed on a movable platform in Chapter 2. Such a system with fixation is a typical example of a strongly-coupled system, in which the perturbation theory fail. We instead defined a lattice model on a moving coordinate, unraveled the quantum classical parts by a coordinate transformation, and straight-forwardly derived an ideal coupling Hamiltonian.

The model discussed in Chapter 3 contains no explicit classical degrees of freedom and does not constitute a quantum-classical coupled system. However, to reproduce the results in Chapter 3, we need classical apparatuses for periodically driving the exchange interactions in the magnetic insulator, for generating slightly different initial states, and for measuring the physical quantities. We therefore need to attach classical systems externally to the quantum system in question. Such external systems and the quantum model treated in Chapter 3 should constitute a quantum-classical coupled system as a whole. It also raises the issue of designing the external systems to some classical-to-quantum perturbation or measure a specific physical quantity by quantum-to-classical back-action.

From the above, each of Chapters 2 and 3 makes the following contributions to the framework of quantum-classical coupled systems proposed in Chapter 1. Chapter 2 presents an experimentally inspired example of quantum-classical coupled systems, together with an entire effective Hamiltonian and a renormalized classical equation of motion. Hence, this chapter provides a means of probing a quantum system coupled to a classical system through the classical part. Chapter 3 predicts non-equilibrium dynamics in a class of quantum many-body systems. To reproduce such non-equilibrium dynamics, we need to design a specific classical system and couple it with the quantum system. This chapter, therefore, raises the issue of designing the classical part in a quantum-classical coupled system.

4.2   Discussions and Future Prospects

It would be interesting to compare our concept of quantum-classical coupled systems with similar studies. In Chapter 2, we treated both two-dimensional

[4]He and a movable platform as a quantum system according to the method proposed in Ref. [57]. It is indeed a way of composing a quantum-classical coupled system. However, according to some methodological studies [94–98], we should be cautious about such a composition. First, there are two natural properties that a quantum-classical coupled system must satisfy: the two systems evolve in time independently and correctly when uncoupled; the equation of motion for the two systems are subject to nontrivial modifications due to the coupling. Methodological studies of quantum-classical coupling date back to Anderson's proposal in Ref. [94], which claimed to satisfy such properties. Unfortunately, it turned out that quantum-to-classical back-action does not occur in his formulation [95, 96], and other studies have shown the same shortcoming in a mathematically rigorous manner [97, 98]. However, it turned out that a more technical approach eliminates this problem and allows us to incorporate quantum-to-classical back-action properly [99–102]. We may need to show that our method is equivalent to the methods proposed in Refs. [94, 99–102] in the next.

It would also be interesting to apply our concept of quantum-classical coupled systems to more fundamental problems, such as quantum thermodynamics and quantum information. One example is a quantum autonomous machine [103–107], which is coupled only to two heat baths. It behaves like a quantum heat engine subjected to external driving. In such a system, the quantum system should have a strong back-action on each heat bath, leading to the idea of probing the quantum system only from the behavior of the heat baths. Another example is a driven dissipative system with a heat bath and a driver [7–9, 108–116]. In the context of the driven dissipative system, one often assumes that the heat bath has dynamical variables, while the driver does not. Such a driver without dynamical variables approximates a system in which the

74

back-action received from the quantum system is infinitely small. To justify this approximation, we have to formulate all external systems as heat baths with degrees of freedom and derive a similar model. Our framework may also be useful for such justification studies.

Bibliography

[1] F. Schäfer, T. Fukuhara, S. Sugawa, Y. Takasu, and Y. Takahashi, Nat. Rev. Phys. **2**, 411 (2020).

[2] K.-D. Wu, Y. Yuan, G.-Y. Xiang, C.-F. Li, G.-C. Guo, and M. Perarnau-Llobet, Sci. Adv. **5**, eaav4944 (2019).

[3] J. Cripe, T. Cullen, Y. Chen, P. Heu, D. Follman, G. D. Cole, and T. Corbitt, Phys. Rev. X **10**, 031065 (2020).

[4] Á. Rivas, Phys. Rev. Lett. **124**, 160601 (2020).

[5] H. Walther, B. T. H. Varcoe, B.-G. Englert, and T. Becker, Rep. Prog. Phys. **69**, 1325 (2006).

[6] J. M. Raimond, M. Brune, and S. Haroche, Rev. Mod. Phys. **73**, 565 (2001).

[7] S. Restrepo, J. Cerrillo, V. M. Bastidas, D. G. Angelakis, and T. Brandes, Phys. Rev. Lett. **117**, 250401 (2016).

[8] M. Carrega, P. Solinas, M. Sassetti, and U. Weiss, Phys. Rev. Lett. **116**, 240403 (2016).

[9] M. C. Goorden, M. Thorwart, and M. Grifoni, Phys. Rev. Lett. **93**, 267005 (2004).

[10] A. H. Castro Neto, F. Guinea, N. M. R. Peres, K. S. Novoselov, and A. K. Geim, Rev. Mod. Phys. **81**, 109 (2009).

[11] M. A. H. Vozmediano, M. I. Katsnelson, and F. Guinea, Physics Reports **496**, 109 (2010).

[12] F. de Juan, J. L. Mañes, and M. A. H. Vozmediano, Phys. Rev. B **87**, 165131 (2013).

[13] L. Tapasztó, T. Dumitrică, S. J. Kim, P. Nemes-Incze, C. Hwang, and L. P. Biró, Nat. Phys. **8**, 739 (2012).

[14] D.-B. Zhang, E. Akatyeva, and T. Dumitrică, Phys. Rev. Lett. **106**, 255503 (2011).

[15] F. Guinea, Solid State Communications **152**, 1437 (2012).

[16] C. Si, Z. Sun, and F. Liu, Nanoscale **8**, 3207 (2016).

[17] I. Y. Sahalianov, T. M. Radchenko, V. A. Tatarenko, G. Cuniberti, and Y. I. Prylutskyy, Journal of Applied Physics **126**, 054302 (2019).

[18] S. H. Mousavi, P. T. Rakich, and Z. Wang, ACS Photonics **1**, 1107 (2014).

[19] T. Zhang, H. Chang, Y. Wu, P. Xiao, N. Yi, Y. Lu, Y. Ma, Y. Huang, K. Zhao, X.-Q. Yan, Z.-B. Liu, J.-G. Tian, and Y. Chen, Nat. Photonics **9**, 471 (2015).

[20] M. M. Salary, S. Inampudi, K. Zhang, E. B. Tadmor, and H. Mosallaei, Phys. Rev. B **94**, 235403 (2016).

[21] A. V. Chumak, V. I. Vasyuchka, A. A. Serga, and B. Hillebrands, Nat. Phys. **11**, 453 (2015).

[22] S. M. Rezende, A. Azevedo, and R. L. Rodríguez-Suárez, Journal of Applied Physics **126**, 151101 (2019).

[23] A. H. MacDonald and M. Tsoi, Phil. Trans. R. Soc. A. **369**, 3098 (2011).

[24] V. Baltz, A. Manchon, M. Tsoi, T. Moriyama, T. Ono, and Y. Tserkovnyak, Rev. Mod. Phys. **90**, 015005 (2018).

[25] J. Linder and J. W. A. Robinson, Nat. Phys. **11**, 307 (2015).

[26] G. Fabiani and J. Mentink, SciPost Phys. **7**, 004 (2019).

[27] F. W. Hehl and W.-T. Ni, Phys. Rev. D **42**, 2045 (1990).

[28] S. J. Barnett, Phys. Rev. **6**, 239 (1915).

[29] M. Matsuo, J. Ieda, K. Harii, E. Saitoh, and S. Maekawa, Phys. Rev. B **87**, 180402 (2013).

[30] J. Fujimoto and M. Matsuo, Phys. Rev. B **102**, 020406 (2020).

[31] A. Einstein, Naturwissenschaften **3**, 237 (1915).

[32] P. Mohanty, G. Zolfagharkhani, S. Kettemann, and P. Fulde, Phys. Rev. B **70**, 195301 (2004).

[33] G. Zolfagharkhani, A. Gaidarzhy, P. Degiovanni, S. Kettemann, P. Fulde, and P. Mohanty, Nat. Nanotechnol. **3**, 720 (2008).

[34] M. F. O'Keeffe, E. M. Chudnovsky, and D. A. Garanin, Phys. Rev. B **87**, 174418 (2013).

[35] A. A. Kovalev, L. X. Hayden, G. E. W. Bauer, and Y. Tserkovnyak, Phys. Rev. Lett. **106**, 147203 (2011).

[36] D. A. Garanin and E. M. Chudnovsky, Phys. Rev. B **92**, 024421 (2015).

[37] A. Polkovnikov, K. Sengupta, A. Silva, and M. Vengalattore, Rev. Mod. Phys. **83**, 863 (2011).

[38] A. Schmitt, *Introduction to superfluidity – Field-theoretical approach and applications*, (July 31, 2014) http://arxiv.org/abs/1404.1284 (visited on 11/20/2020).

[39] S. I. Vilchynskyy, A. I. Yakimenko, K. O. Isaieva, and A. V. Chumachenko, Low Temperature Physics **39**, 724 (2013).

[40] D. Vollhardt and P. Woelfle, *Superfluid Helium 3: Link between Condensed Matter Physics and Particle Physics*, (Dec. 5, 2000) `http://arxiv.org/abs/cond-mat/0012052` (visited on 11/20/2020).

[41] J. Day and J. Beamish, J Low Temp Phys **148**, 627 (2007).

[42] A. Haziot, A. D. Fefferman, F. Souris, J. R. Beamish, H. J. Maris, and S. Balibar, Phys. Rev. B **88**, 014106 (2013).

[43] S. Nakamura, K. Matsui, T. Matsui, and H. Fukuyama, Phys. Rev. B **94**, 180501 (2016).

[44] M. C. Gordillo and J. Boronat, Phys. Rev. Lett. **124**, 205301 (2020).

[45] S. Moroni and M. Boninsegni, Phys. Rev. B **99**, 195441 (2019).

[46] N. Hosomi and M. Suzuki, J Low Temp Phys **148**, 773 (2007).

[47] N. Hosomi, A. Tanabe, M. Suzuki, and M. Hieda, Phys. Rev. B **75**, 064513 (2007).

[48] N. Hosomi and M. Suzuki, Phys. Rev. B **77**, 024501 (2008).

[49] N. Hosomi, J. Taniguchi, M. Suzuki, and T. Minoguchi, Phys. Rev. B **79**, 172503 (2009).

[50] J. Krim, D. H. Solina, and R. Chiarello, Phys. Rev. Lett. **66**, 181 (1991).

[51] A. Dayo, W. Alnasrallah, and J. Krim, Phys. Rev. Lett. **80**, 1690 (1998).

[52] C. Mak and J. Krim, Phys. Rev. B **58**, 5157 (1998).

[53] L. Bruschi, A. Carlin, and G. Mistura, Phys. Rev. Lett. **88**, 046105 (2002).

[54] A. Carlin, L. Bruschi, M. Ferrari, and G. Mistura, Phys. Rev. B **68**, 045420 (2003).

[55] M. Highland and J. Krim, Phys. Rev. Lett. **96**, 226107 (2006).

[56] J. Krim, Adv. Phys. **61**, 155 (2012).

[57] S. E. Korshunov, Jetp Lett. **90**, 156 (2009).

[58] G. Grynberg and C. Robilliard, Physics Reports **355**, 335 (2001).

[59] C. Becker, P. Soltan-Panahi, J. Kronjäger, S. Dörscher, K. Bongs, and K. Sengstock, New J. Phys. **12**, 065025 (2010).

[60] P. Windpassinger and K. Sengstock, Rep. Prog. Phys. **76**, 086401 (2013).

[61] D. Jaksch, C. Bruder, J. I. Cirac, C. W. Gardiner, and P. Zoller, Phys. Rev. Lett. **81**, 3108 (1998).

[62] T. Matsubara and H. Matsuda, Prog Theor Phys **16**, 569 (1956).

[63] H. Matsuda and T. Matsubara, Prog Theor Phys **17**, 19 (1957).

[64] P. Weinberg and M. Bukov, SciPost Phys. **2**, 003 (2017).

[65] P. Weinberg and M. Bukov, SciPost Phys. **7**, 020 (2019).

[66] P. A. Whitlock, G. V. Chester, and B. Krishnamachari, Phys. Rev. B **58**, 8704 (1998).

[67] P. Corboz, M. Boninsegni, L. Pollet, and M. Troyer, Phys. Rev. B **78**, 245414 (2008).

[68] N. Gheeraert, S. Chester, M. May, S. Eggert, and A. Pelster, in Selforganization in Complex Systems: The Past, Present, and Future of Synergetics, edited by G. Wunner and A. Pelster, Understanding Complex Systems (2016), pp. 289–296.

[69] J. H. Shirley, Phys. Rev. **138**, B979 (1965).

[70] M. Aidelsburger, M. Atala, S. Nascimbène, S. Trotzky, Y.-A. Chen, and I. Bloch, Phys. Rev. Lett. **107**, 255301 (2011).

[71] P. Hauke, O. Tieleman, A. Celi, C. Ölschläger, J. Simonet, J. Struck, M. Weinberg, P. Windpassinger, K. Sengstock, M. Lewenstein, and A. Eckardt, Phys. Rev. Lett. **109**, 145301 (2012).

[72] J. Struck, C. Ölschläger, M. Weinberg, P. Hauke, J. Simonet, A. Eckardt, M. Lewenstein, K. Sengstock, and P. Windpassinger, Phys. Rev. Lett. **108**, 225304 (2012).

[73] M. Aidelsburger, M. Atala, M. Lohse, J. T. Barreiro, B. Paredes, and I. Bloch, Phys. Rev. Lett. **111**, 185301 (2013).

[74] H. Miyake, G. A. Siviloglou, C. J. Kennedy, W. C. Burton, and W. Ketterle, Phys. Rev. Lett. **111**, 185302 (2013).

[75] J. Struck, M. Weinberg, C. Ölschläger, P. Windpassinger, J. Simonet, K. Sengstock, R. Höppner, P. Hauke, A. Eckardt, M. Lewenstein, and L. Mathey, Nat. Phys. **9**, 738 (2013).

[76] M. Atala, M. Aidelsburger, M. Lohse, J. T. Barreiro, B. Paredes, and I. Bloch, Nat. Phys. **10**, 588 (2014).

[77] M. Aidelsburger, S. Nascimbene, and N. Goldman, Comptes Rendus Physique **19**, 394 (2018).

[78] Z. Gu, H. A. Fertig, D. P. Arovas, and A. Auerbach, Phys. Rev. Lett. **107**, 216601 (2011).

[79] A. Kundu, H. A. Fertig, and B. Seradjeh, Phys. Rev. Lett. **113**, 236803 (2014).

[80] P. M. Perez-Piskunow, G. Usaj, C. A. Balseiro, and L. E. F. F. Torres, Phys. Rev. B **89**, 121401 (2014).

[81] X. Zhai and G. Jin, Phys. Rev. B **89**, 235416 (2014).

[82] H. Dehghani, T. Oka, and A. Mitra, Phys. Rev. B **91**, 155422 (2015).

[83] M. A. Sentef, M. Claassen, A. F. Kemper, B. Moritz, T. Oka, J. K. Freericks, and T. P. Devereaux, Nat. Commun. **6**, 7047 (2015).

[84] G. E. Topp, G. Jotzu, J. W. McIver, L. Xian, A. Rubio, and M. A. Sentef, Phys. Rev. Research **1**, 023031 (2019).

[85] J. W. McIver, B. Schulte, F.-U. Stein, T. Matsuyama, G. Jotzu, G. Meier, and A. Cavalleri, Nat. Phys. **16**, 38 (2020).

[86] Á. Rapp, X. Deng, and L. Santos, Phys. Rev. Lett. **109**, 203005 (2012).

[87] F. Meinert, M. J. Mark, K. Lauber, A. J. Daley, and H.-C. Nägerl, Phys. Rev. Lett. **116**, 205301 (2016).

[88] C. J. Turner, A. A. Michailidis, D. A. Abanin, M. Serbyn, and Z. Papić, Phys. Rev. B **98**, 155134 (2018).

[89] C. J. Turner, A. A. Michailidis, D. A. Abanin, M. Serbyn, and Z. Papić, Nat. Phys. **14**, 745 (2018).

[90] P. Weinberg and M. Bukov, SciPost Phys. **2**, 003 (2017).

[91] P. Weinberg and M. Bukov, SciPost Phys. **7**, 020 (2019).

[92] J. H. Mentink, J. Phys.: Condens. Matter **29**, 453001 (2017).

[93] N. M. Temme, *Special functions: an introduction to the classical functions of mathematical physics* (Wiley, New York, 1996), 374 pp.

[94] A. Anderson, Phys. Rev. Lett. **74**, 621 (1995).

[95] K. R. W. Jones, Phys. Rev. Lett. **76**, 4087 (1996).

[96] I. R. Senitzky, Phys. Rev. Lett. **76**, 4089 (1996).

[97] J. Caro and L. L. Salcedo, Phys. Rev. A **60**, 842 (1999).

[98] D. Sahoo, J. Phys. A: Math. Gen. **37**, 997 (2004).

[99] L. L. Salcedo, Phys. Rev. A **85**, 022127 (2012).

[100] C. Barceló, R. Carballo-Rubio, L. J. Garay, and R. Gómez-Escalante, Phys. Rev. A **86**, 042120 (2012).

[101] V. Gil and L. L. Salcedo, Phys. Rev. A **95**, 012137 (2017).

[102] M. Amin and M. Walton, *Quantum-Classical Dynamical Brackets*, (Oct. 21, 2020) http://arxiv.org/abs/2009.09573 (visited on 10/30/2020).

[103] F. Tonner and G. Mahler, Phys. Rev. E **72**, 066118 (2005).

[104] J. Teifel and G. Mahler, Phys. Rev. E **83**, 041131 (2011).

[105] J. B. Brask, G. Haack, N. Brunner, and M. Huber, New J. Phys. **17**, 113029 (2015).

[106] M. F. Frenzel, D. Jennings, and T. Rudolph, New J. Phys. **18**, 023037 (2016).

[107] C. Wang and J. M. Gertler, Phys. Rev. Research **1**, 033198 (2019).

[108] S. Kohler, T. Dittrich, and P. Hänggi, Phys. Rev. E **55**, 300 (1997).

[109] M. Grifoni and P. Hänggi, Physics Reports **304**, 229 (1998).

[110] J. Eckel, J. H. Reina, and M. Thorwart, New J. Phys. **11**, 085001 (2009).

[111] D. W. Hone, R. Ketzmerick, and W. Kohn, Phys. Rev. E **79**, 051129 (2009).

[112] P. Talkner and P. Hänggi, Rev. Mod. Phys. **92**, 041002 (2020).

[113] J. Hausinger and M. Grifoni, Phys. Rev. A **81**, 022117 (2010).

[114] K. Szczygielski, D. Gelbwaser-Klimovsky, and R. Alicki, Phys. Rev. E **87**, 012120 (2013).

[115] K. Szczygielski, Journal of Mathematical Physics **55**, 083506 (2014).

[116] C. Chen, J.-H. An, H.-G. Luo, C. P. Sun, and C. H. Oh, Phys. Rev. A **91**, 052122 (2015).